A Light for Science

ESRF

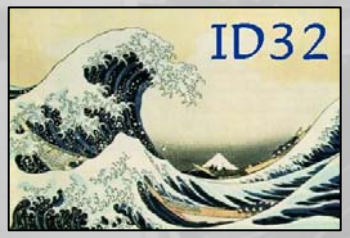

European Synchrotron Radiation Facility

X-ray Standing Waves and HAXPES at the ID32 beamline

Jörg Zegenhagen

ESRF Grenoble, France

X-ray Standing Waves and HAXPES at the ID32 beamline

- The ID32 beamline
- X-ray standing waves (XSW)
- XSW combined with photoelectron spectrocopy
  - Chemical shift: Organic molecules on surfaces, root(3) structure of Sn on Ge(111)
  - Element specific XSW imaging: Nucleation of a superconductor $YBa_2Cu_3O_{7-\delta}$ on $SrTiO_3(001)$
  - "Localizing" valence electrons: XSW valence band spectroscopy of $SrTiO_3$
- XSW, PE and limit of dipole approximation
- New HAXPES set-up at ID32 → *Latest results: see poster by Blanka Detlefs*
- Conclusions & Outlook

Insertion device beamline ID32

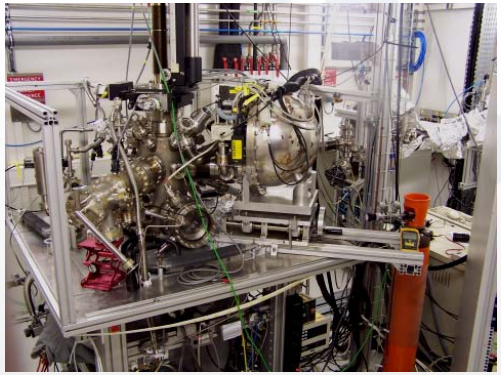

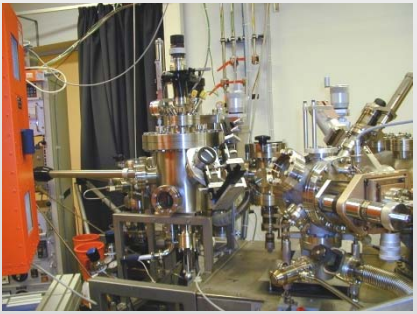

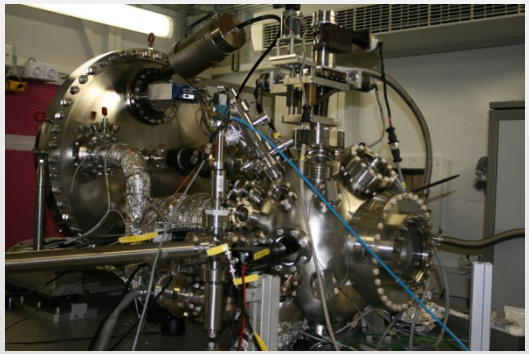

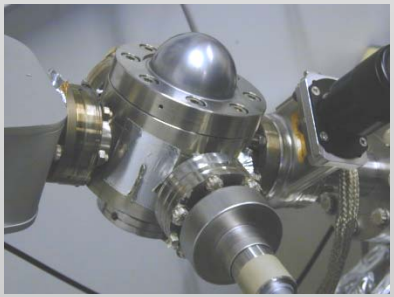

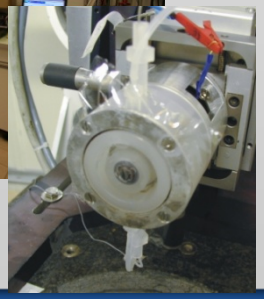

Energy range: *(1.0) 2.0 – 30 keV*

Three undulators, 11 mm gap: **2xU35, 1xU42**

Photon flux: *> 10 ^{13} photons/sec*

Beam size (focused): *30 x 300 μm^2 (with CRL)*

min. ca. V x H = 1 x 10μm^2 (with zone plate)

Fixed offset mono, Si(111) and multilayer

Two postmonos → $10^{-6} < \Delta E/E < 10^{-4}$

Two experimental hutches

Experimental hutch 1:

- *(S)XRD + XSW*

  (multi-purpose six-circle kappa diffractometer)

Experimental hutch 2 :

- *XSW + XPS*

  UHV system 1:

  PHI electron analyzer, max. K.E. = 4.8 keV

  UHV system 2** (since 2008)**:

  SPECS PHOIBOS 225, max. K.E. = 15 keV,

  High energy resolution

Two associated laboratories

- *Surface Characterization Lab*

  (MBE, PLD, STM, LEED, Auger, ...)

  and baby chambers

- *Electrochemistry Lab (since 2008)*

  potentiostats etc. and in situ cells

HAXPES activities at ID32

- HAXPES of buried interfaces (basic and applied research)
- Cross sections, elastic mean free path, intrinsic and extrinsic excitations →e.g.: *Outer Sub-Shell Cross-Sections Determined by X-ray Photoelectron Spectroscopy up to 14.5 keV*, C. Kunz, S. Thiess, B.C.C. Cowie, T.-L. Lee, and J. Zegenhagen, Nuclear Instruments and Methods A 547, 73–86 (2005); *Relative electron inelastic mean free paths for diamond and graphite at 8 keV and intrinsic contributions to the energy-loss*, C. Kunz, B.C.C. Cowie,W. Drube, T.-L. Lee, S. Thiessc, C. Wilde, J. Zegenhagen, J. Electron Spectrosc. Relat. Phenom. (2009), doi:10.1016/j.elspec.2009.03.022
- HAXPES and X-rays standing waves

X-ray standing wave – an interference field

$$\mathbf{E}_{\text{total}}(\mathbf{r},t) = \mathbf{E}_1 \cos(\mathbf{k}_1 \cdot \mathbf{r} - \omega t) + \mathbf{E}_2 \cos(\mathbf{k}_2 \cdot \mathbf{r} - \omega t + \varphi)$$

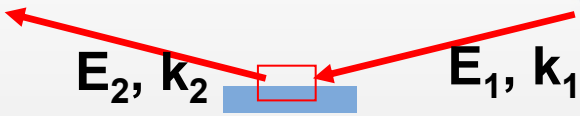

$$|\mathbf{k}_1| = |\mathbf{k}_2| = \frac{2\pi}{\lambda}$$

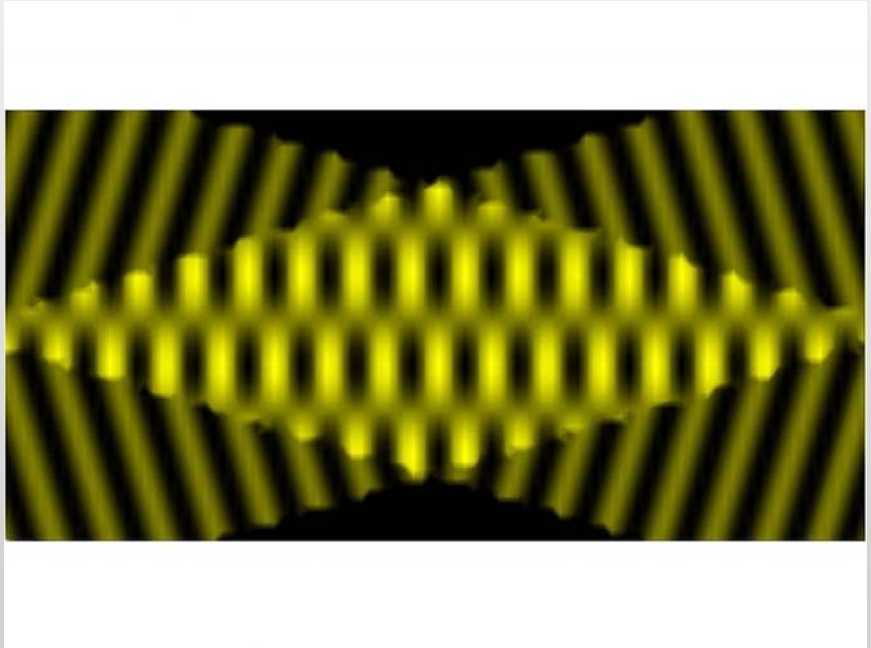

$\varphi = 0$

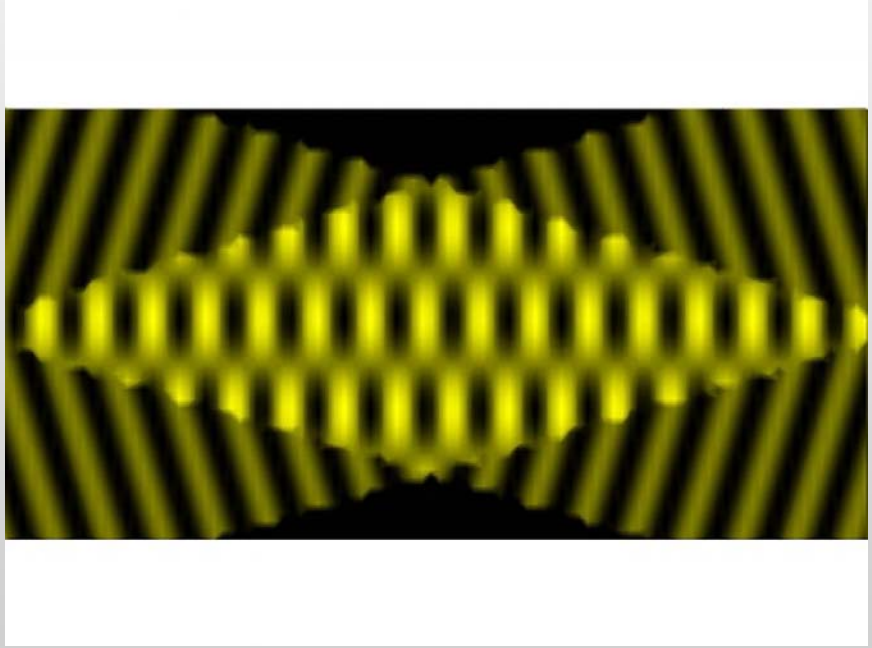

$\varphi = \pi$

Photoexcitation by the X-ray standing wave

$$\mathbf{E}_{\text{total}}(\mathbf{r},t) = \mathbf{E}_1 \cos(\mathbf{k}_1 \cdot \mathbf{r} - \omega t) + \mathbf{E}_2 \cos(\mathbf{k}_2 \cdot \mathbf{r} - \omega t + \varphi)$$

$$|\mathbf{k}_1| = |\mathbf{k}_2| = \frac{2\pi}{\lambda}$$

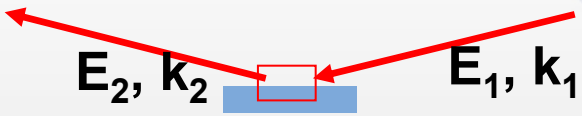

Atoms with their center at the maxima of The wavefield will experience strong photoabsorption and consequently Radiate strongly whereas the atoms at the Minima of the wavefield remain “invisible”

→ Standing Wave Intensity:

$$I = 1 + R + 2\sqrt{R}\cos(\varphi - 2\pi\mathbf{Hr})$$

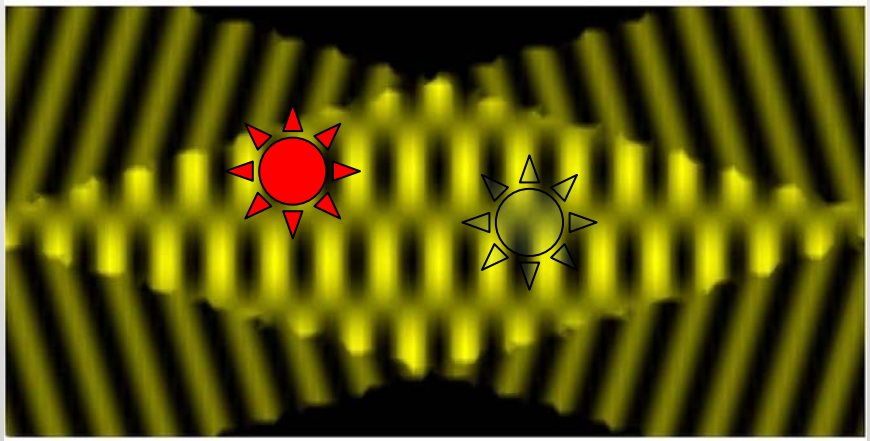

$\varphi = 0$

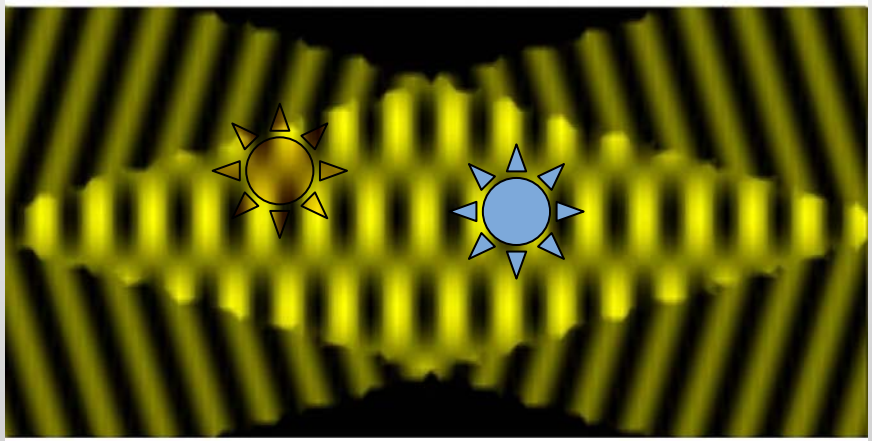

$\varphi = \pi$

Photoexcitation and dipole approximation

Perturbation theory gives the transition matrix element for photoabsorption:

The photoelectric absorption or Photoelectron emission is Proportional to the transition Matrix element $\mathbf{M_{fi}}$

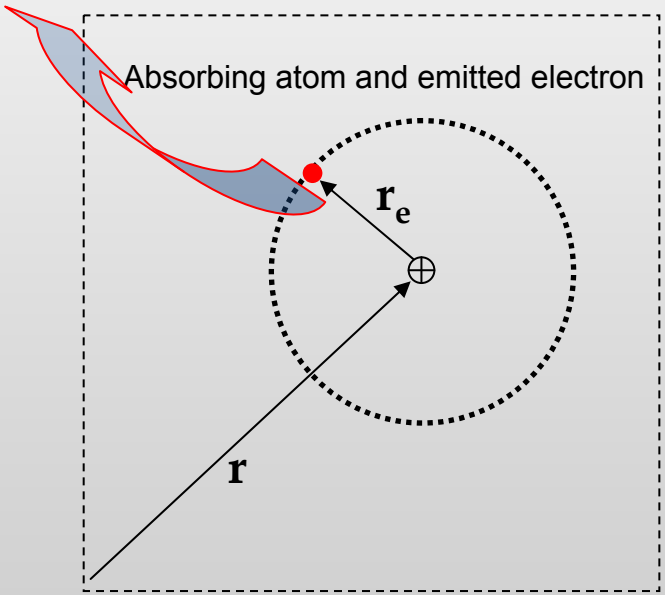

Reference frame, e.g., crystal unit cell

$$\mathbf{M_{fi}} \propto \int d^3R\, \psi_f^* \mathbf{Ap}\, \psi_\mathbf{i}$$

$\mathbf{A}$ is the vector potential of the X-ray wave field,

$$\mathbf{A} = \mathbf{A_0} e^{-2\pi i \mathbf{K_0 R}} (\overrightarrow{E_0} + \overrightarrow{E_H} \sqrt{R} e^{i\varphi} e^{-2\pi i \mathbf{HR}})$$

polaris. vectors $\overrightarrow{E_0}, \overrightarrow{E_H}$

$\mathbf{R} = \mathbf{r_e} + \mathbf{r}$, $\mathbf{r}$ = atom position, $\mathbf{r_e}$ = electron position

$$\mathbf{A} = \mathbf{A_0} e^{-2\pi i \mathbf{K_0 r}} e^{-2\pi i \mathbf{K_0 r_e}} (\overrightarrow{E_0} + \overrightarrow{E_H} \sqrt{R} e^{i\varphi} e^{-2\pi i \mathbf{Hr}} e^{-2\pi i \mathbf{Hr}_e})$$

Multipole expansion :

$$e^{-2\pi i \mathbf{K_0 r_e}} = 1 - 2\pi i \mathbf{K_0 r_e} + 2\pi^2 (\mathbf{K_0 r_e})^2 - \ldots$$

$$e^{-2\pi i \mathbf{Hr_e}} = 1 - 2\pi i \mathbf{Hr_e} + 2\pi^2 (\mathbf{Hr_e})^2 - \ldots$$

Dipole approx. (only first term) :

$e^{-2\pi i \mathbf{K_0 r_e}} = e^{-2\pi i \mathbf{Hr_e}} = 1$, thus we obtain

$$\mathbf{A} = \mathbf{A_0} e^{-2\pi i \mathbf{K_0 r}} (\overrightarrow{E_0} + \overrightarrow{E_H} \sqrt{R} e^{i\varphi} e^{-2\pi i \mathbf{Hr}})$$

electron position $\mathbf{r_e}$ has vanished

Photoelectron yield from atom within X-ray standing wave

Wavefield spacing:

$$ds = H^{-1} \text{ with } H = |\mathbf{H}|$$

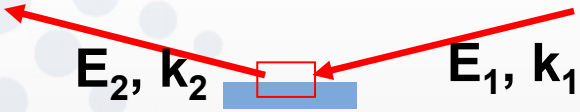

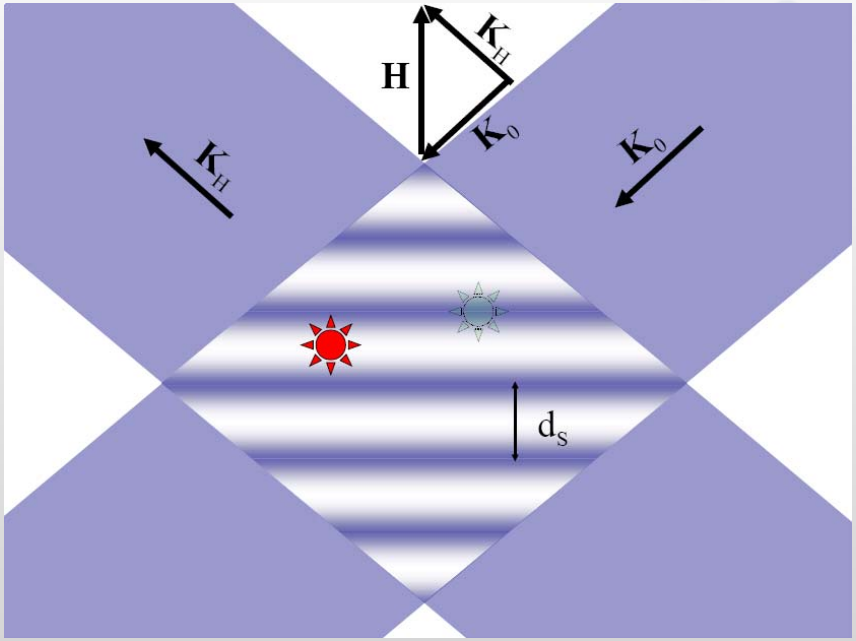

Wavefield intensity:

$$I = 1 + R + 2\sqrt{R}\cos(\varphi - 2\pi\mathbf{Hr})$$

Dipole approximation →
Photoelectron yield from single atom:

$$Y = 1 + R + 2\sqrt{R}\cos(\varphi - 2\pi\mathbf{Hr})$$

Photoelectron yield from N atoms:

$$Y = 1/N\sum_{N}\{1 + R + 2\sqrt{R}\cos(\varphi - 2\pi\mathbf{Hr}_i)\} = 1 + R + 2\sqrt{R}F\cos(\varphi - 2\pi P)$$

P is the normalized (average) position (0 < P < 1) projected along the direction of H

X-ray standing waves in / on single crystals

Photoelectron, fluorescence yield

$$I_{SC} = I_{OB}[1 + R + 2\sqrt{R}F^{\mathbf{H}}\cos(\varphi - 2\pi P^{\mathbf{H}})]$$

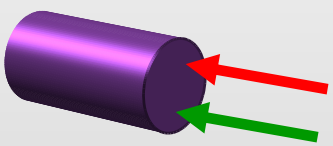

X-ray fluorescence
Auger electrons
Photoelectrons
...

$\propto |\boldsymbol{E}|^2$

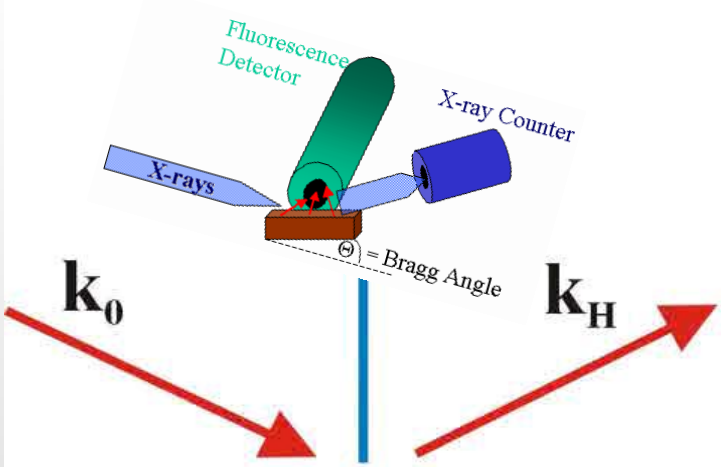

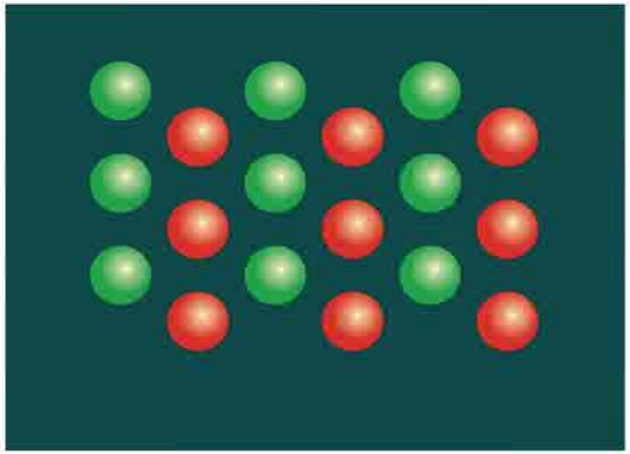

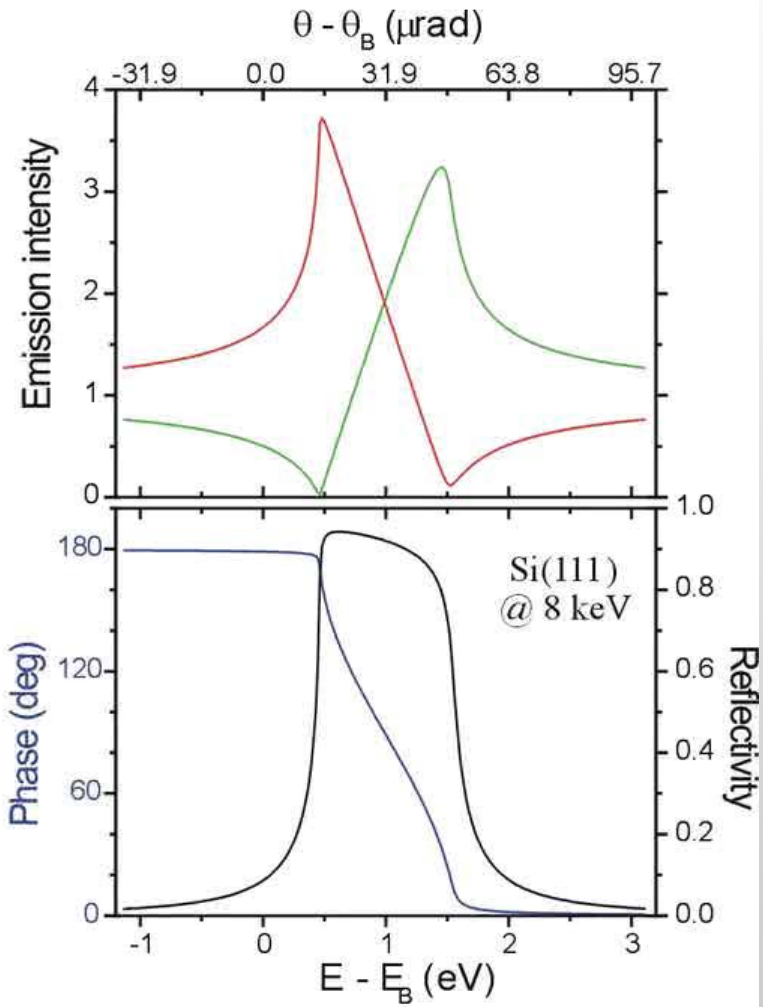

XSW result: Simple interpretation of coherent position P

One reflection ***H*** = [hkl] yields "one position" P^H normal to planes (hkl)
$P^H = \Delta d_H / d_H$, Utilizing several reflections 3D positions can be obtained by "triangulation", e.g., as shown for an forein atom on GaAs(001)

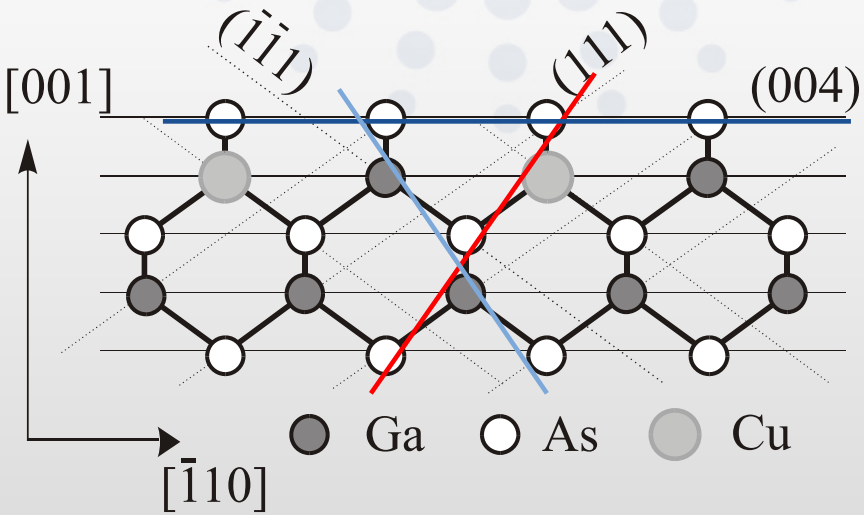

$$I_{PE} = I_{OB}[1 + R + 2\sqrt{R}F^{\mathbf{H}}\cos(\varphi - 2\pi P^{\mathbf{H}})]$$

At this point, the coherent fraction F^H is neglected

In-situ XSW Study of electrodeposited Cu on n-type GaAs(001)

XSW, (004) reflection

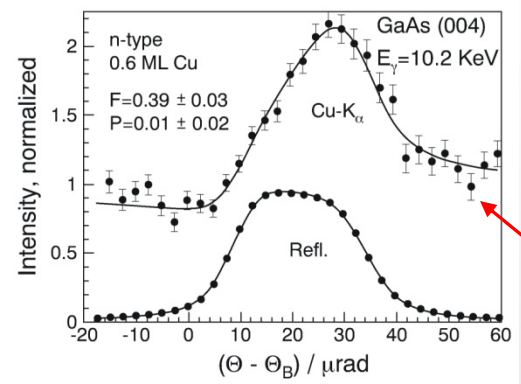

0.8 ML Cu on GaAs(001)

XSW, (111) reflection

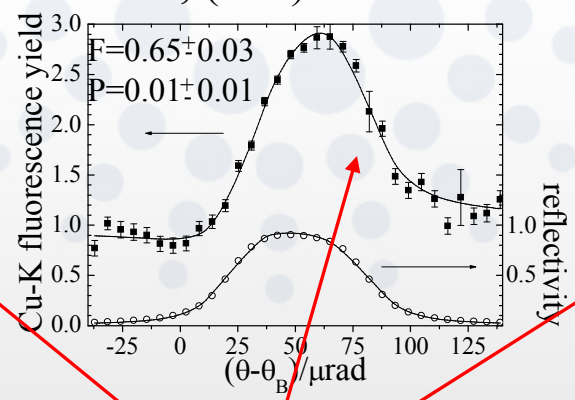

1 ML Cu on GaAs(001)

XSW, (-1-1-1) reflection

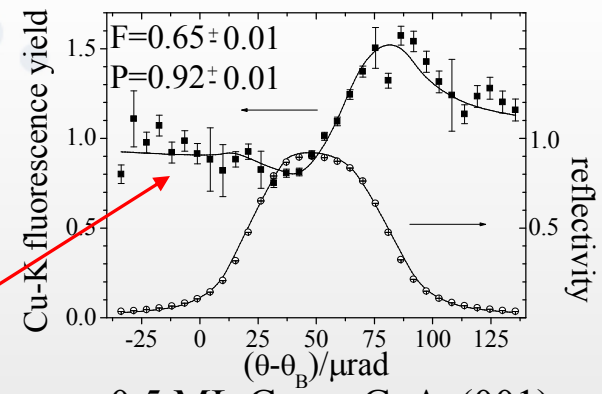

0.5 ML Cu on GaAs(001)

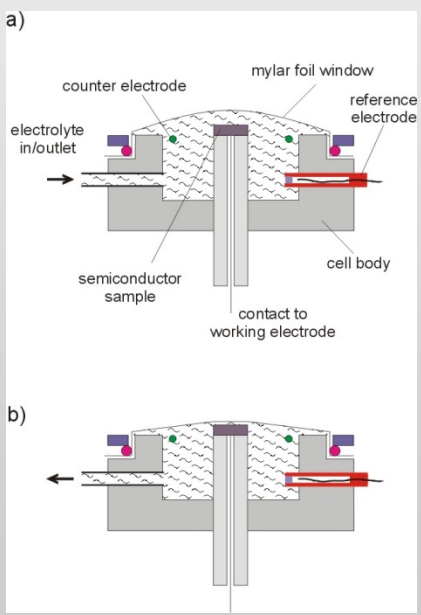

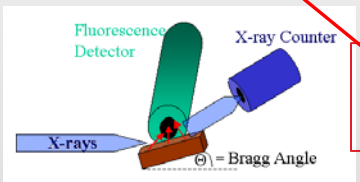

$$I_{SC} = I_{OB}[1 + R + 2\sqrt{R}F^{\mathbf{H}}\cos(\varphi - 2\pi P^{\mathbf{H}})$$

The distance z_H of Cu Atoms to the GaAs planes is directly measured: $z_H = P^H/d_H$

d_H = plane spacing

Cu is located mostly on substitutional (Ga) lattice sites.

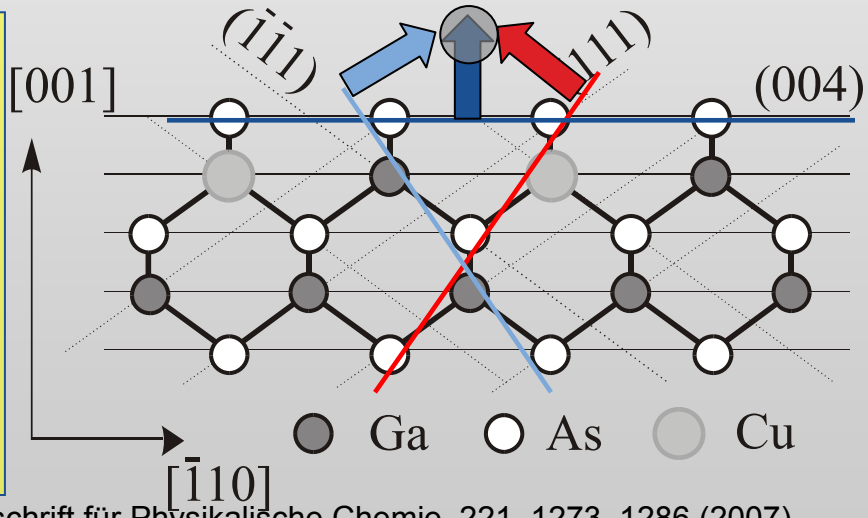

J. Zegenhagen, T.-L. Lee, Y. Gründer, F. Renner, B.-O. Fimland, Zeitschrift für Physikalische Chemie. 221, 1273–1286 (2007).

XSW/XPS setup at beamline ID32

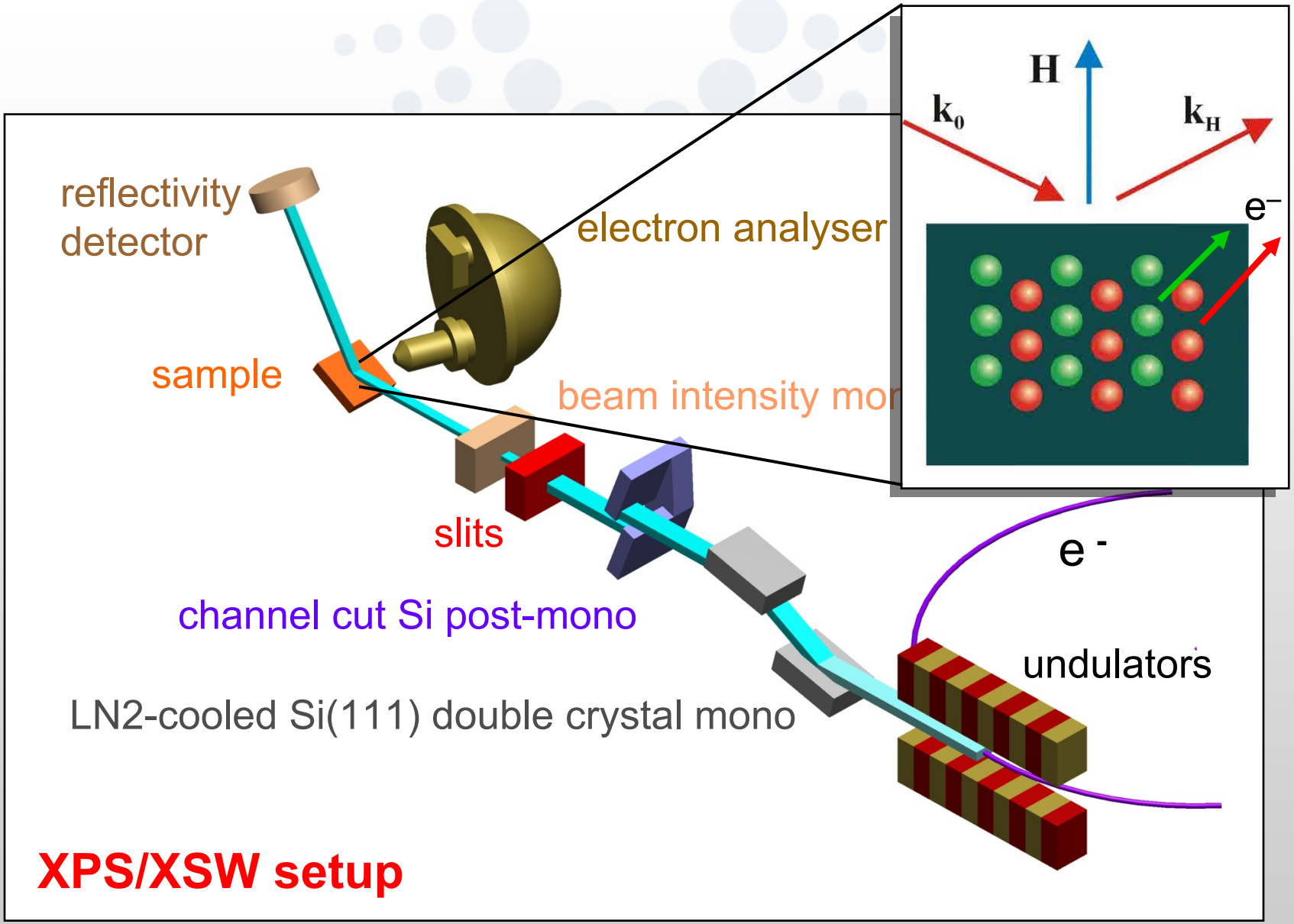

XPS/XSW setup

X-ray photoelectron spectroscopy under the influence of an X-ray standing wave (XSW):

Chemical and electronic properties of condensed matter
➔ Site specific

From attractive to repulsive intermolecular interaction: A reversible phase transition in an ordered organic sub-monolayer film: Sn-Phthalocyanine on Ag(111)

Christoph Stadler et al., Nature Physics 2009

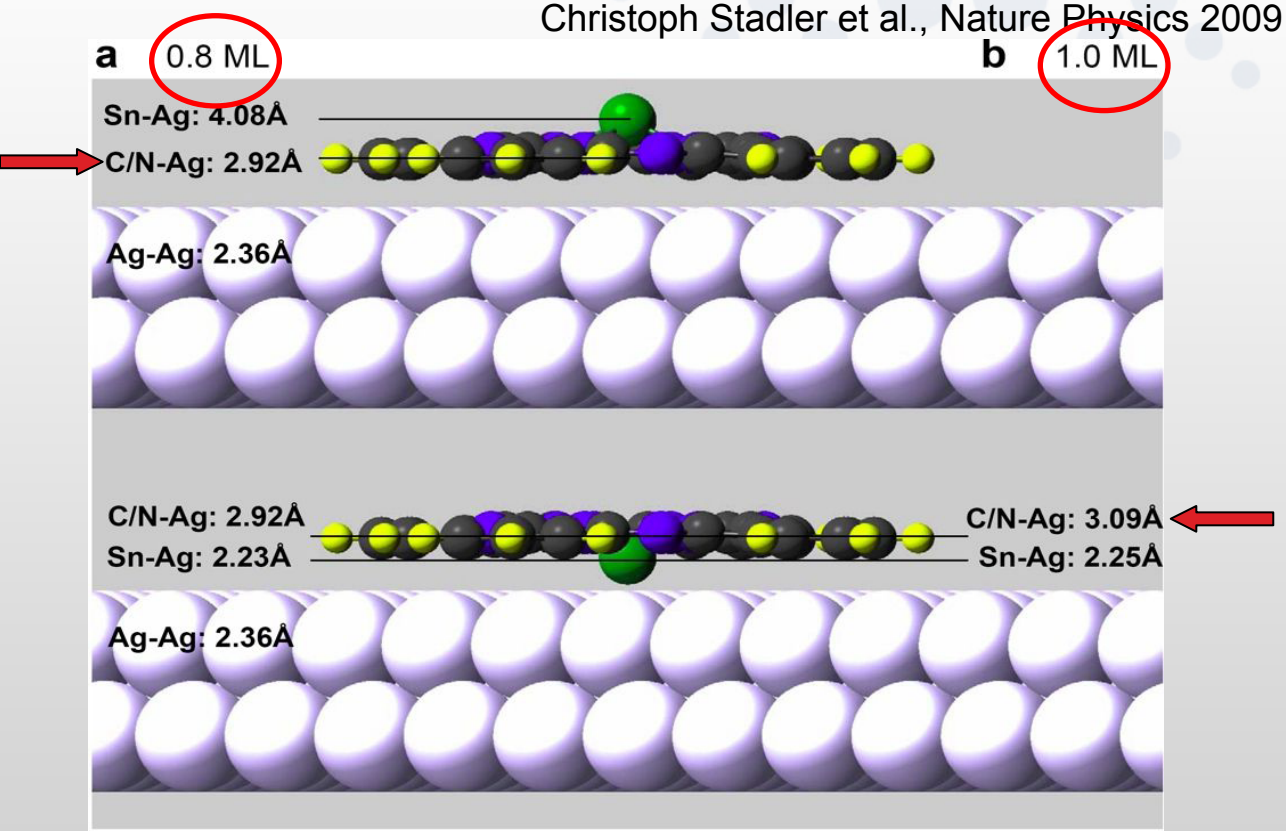

Results of the XSW measurements (schematic). Side views of a molecule with Sn-up (upper part of the figure) and Sn-down position (lower part) are shown. The heights for C and N atoms are identical.
(a) Left side: Coverage of 0.8 ML; In this case Sn-up and Sn-down oriented molecules are present (Sn-Ag distances of 4.08 Å and 2.23 Å).
(b) Coverage of 1.0 ML; only Sn-down oriented molecules are present. **The C/N-Ag distance is enlarged, indicating a weaker molecule-substrate interaction due to a stronger (substrate- mediated) repulsion between the molecules.**

With increasing coverage Sn-Phthalocyanine molecules continuously rearrange on a Ag(111) surface in a series of *ordered* superstructures and – at all coverages – fill the entire surface homogenously.

Motivation

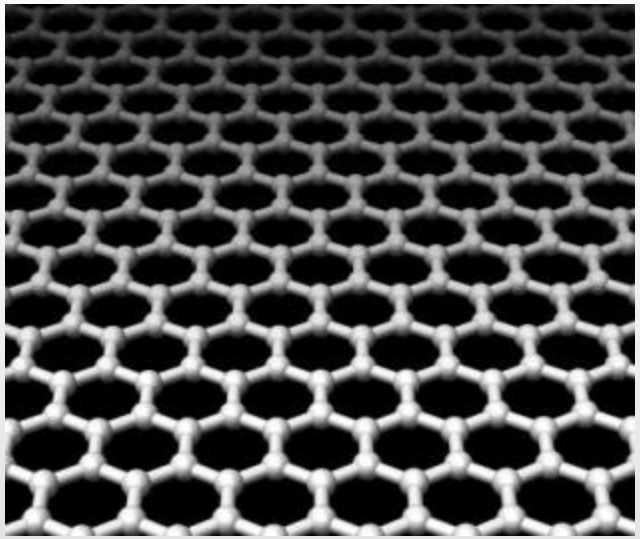

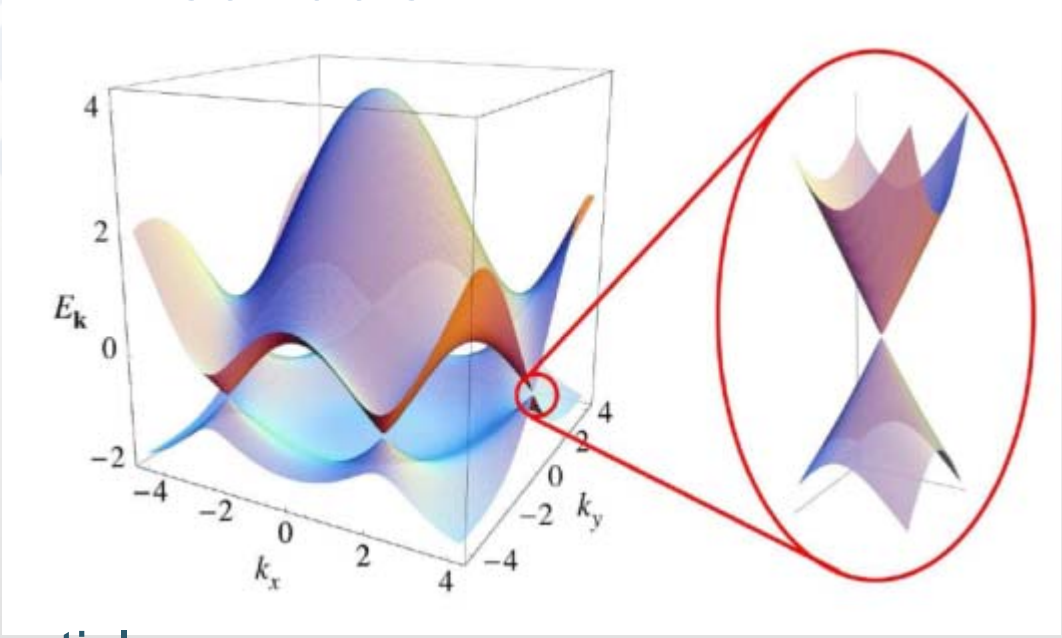

- electrons behave like Dirac-particles
- interesting for applications:
  - huge mobility
  - ballistic transport
  - large spin coherence length
  - transparent but conducting

Courtesy: Carsten Busse, Univ. Cologn

Chemical vapor deposition (CVD) on Ir(111)

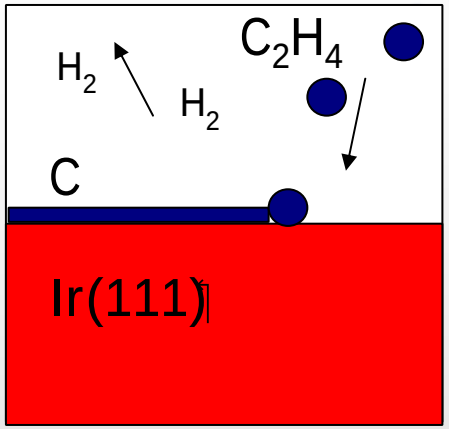

(800-1500 K)

growth of up to 1 ML,
but not more (self limiting)

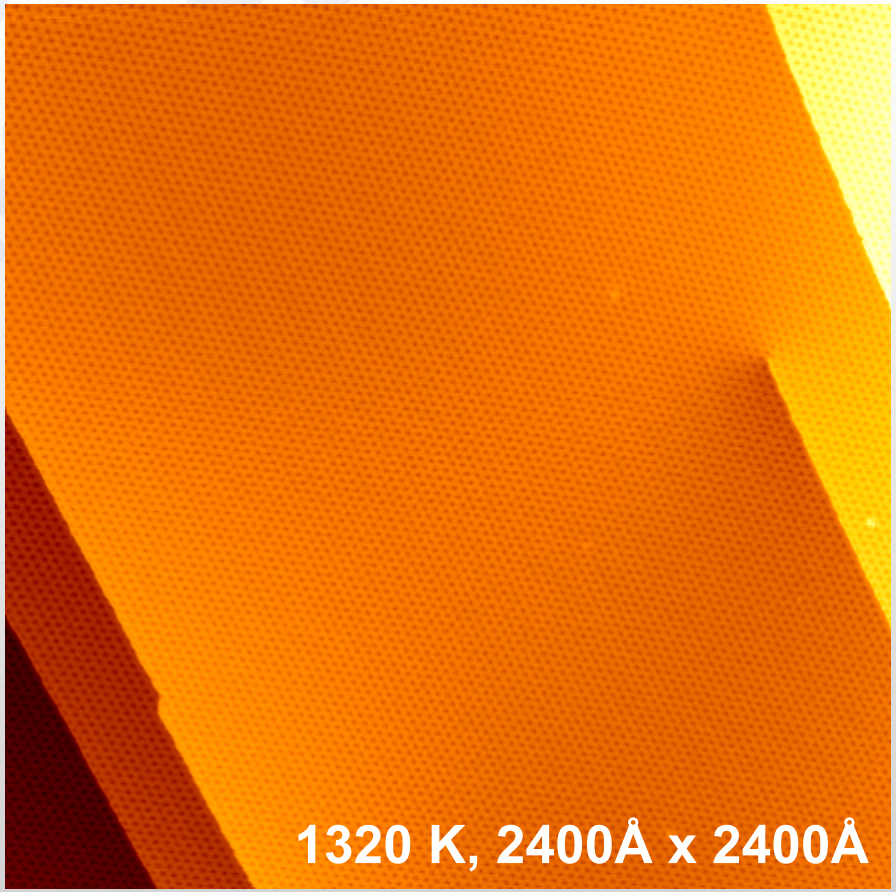

J. Coraux, A. T. N'Diaye, M. Engler, C. Busse, D. Wall, N. Buckanie, F.-J. Meyer zu Heringdorf, R. van Gastel, B. Poelsema, T. Michely, New J. Phys. **11**, 023006 (2009)

Courtesy: Carsten Busse, Univ. Cologn

Moiré structure

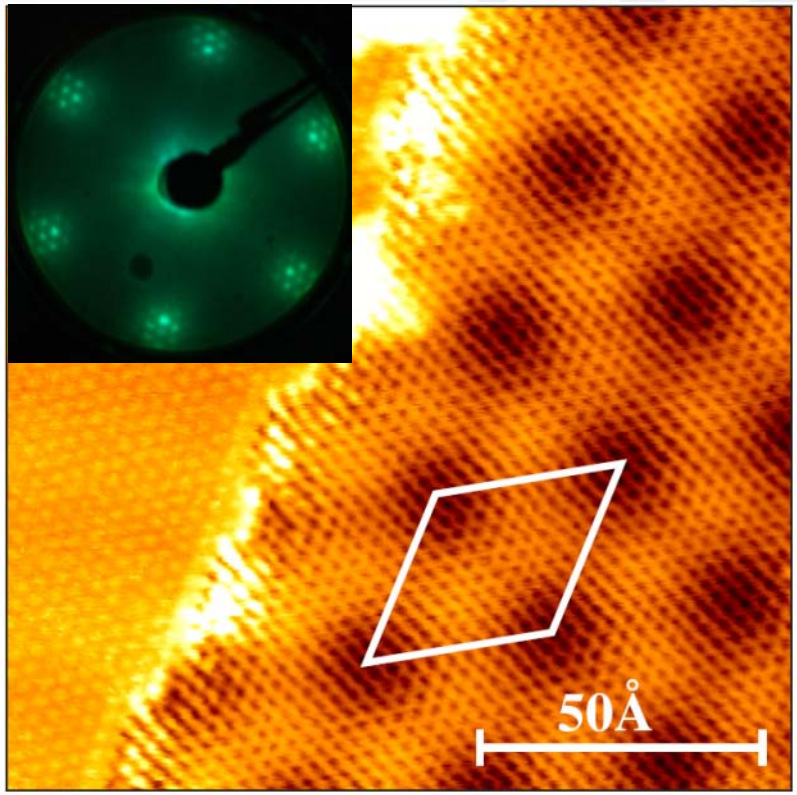

Moiré analysis [1]:

$a_{Graphene}$ = (2.452 ± 0.004) Å

comp.: $a_{Graphite}$ = 2.461 Å

$a_{Moiré}$ = (25.3 ± 0.4) Å

≈ 87 Ir atoms

(incommensurate 9.32 × 9.32)

DFT calculation (no vdW) [2]

$h_{graphene}$= 3.42 Å (LDA)

[1] A. T. N'Diaye, J. Coraux, T. N. Plasa, C. Busse, T. Michely, New J. Phys. **10**, 043033 (2008)
[2] A. T. N'Diaye, S. Bleikamp, P. J. Feibelman, T. Michely, Phys. Rev. Lett. **97**, 215501 (2006)

Courtesy: Carsten Busse, Univ. Cologn

XSW/HAXPES analysis of graphene on Ir(111)

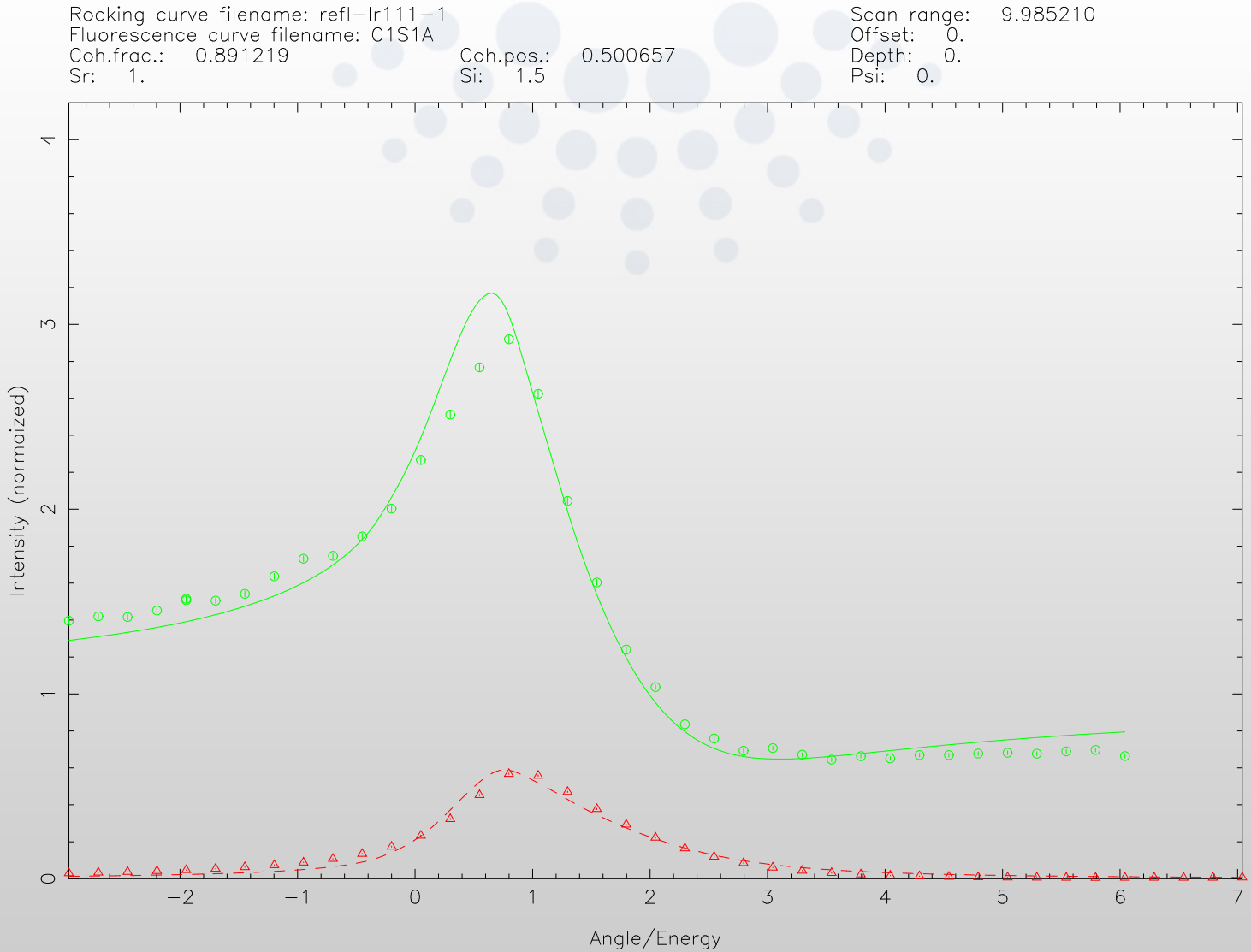

C. Busse, R. Djemour, T. Gerber, A. T. N'Diaye, T. Michely (Universität zu Köln) and J. Coraux (CNRS, Grenoble)

XSW/HAXPES analysis of graphene on Ir(111)

- First preliminary analysis shows that graphene on Ir(111) forms indeed an extremely flat, van der Waals bound, 2 dimensional crystal (layer)

Beyond element specificity

- Probing chemical states through core-level binding energy shifts

Electron Spectroscopy for chemical analysis ESCA

Kai Siegbahn

Ethyl trifluoroacetate

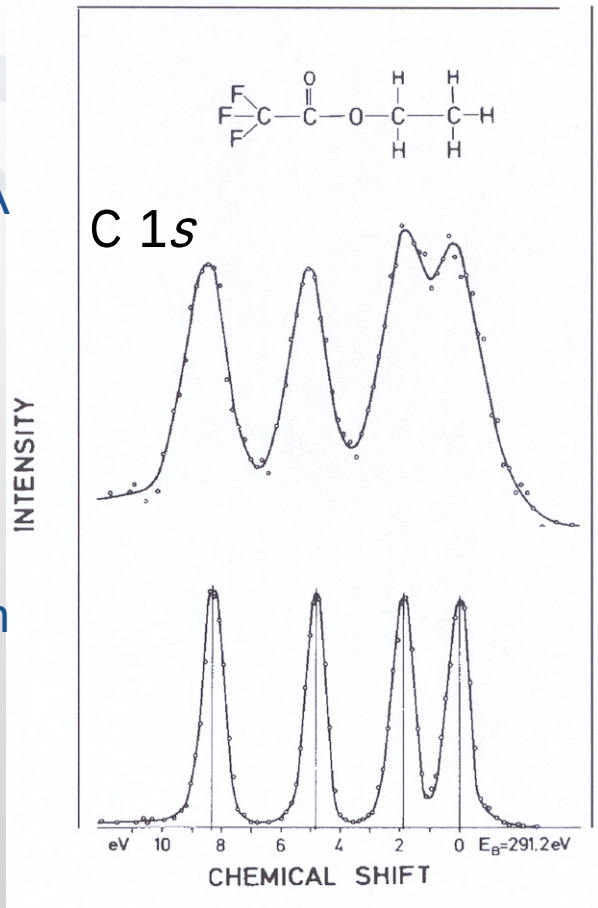

U. Gelius, E. Basilier, S. Svensson, T. Bergmark and K. Siegbahn, J. Electron Sepectrosc. **2**, *405 (1974)*

Combine core-level shift detection with XSW:

M. Sugiyama, S. Maeyama, S. Heun, and M. Oshima, PRB **51**, *14778 (1995) – Sulfur passivated GaAs(001)*

G.J. Jackson, D.P. Woodruff, R.G. Jones, N.K. Singh, A.S.Y. Chan, B.C.C. Cowie, and V. Formoso, PRL **84**, *119 (2000) – CH_3SH/Cu(111)*

Molecular Distortions and Chemical Bonding of PTCDA/Ag(111)

*A. Hauschild, K. Karki, B. C. C. Cowie, M. Rohlfing, F. S. Tautz, and M. Sokolowski, PRL **94**, 036106 (2005)*

3,4,9,10-perylene-tetracarboxylic-dianhydride

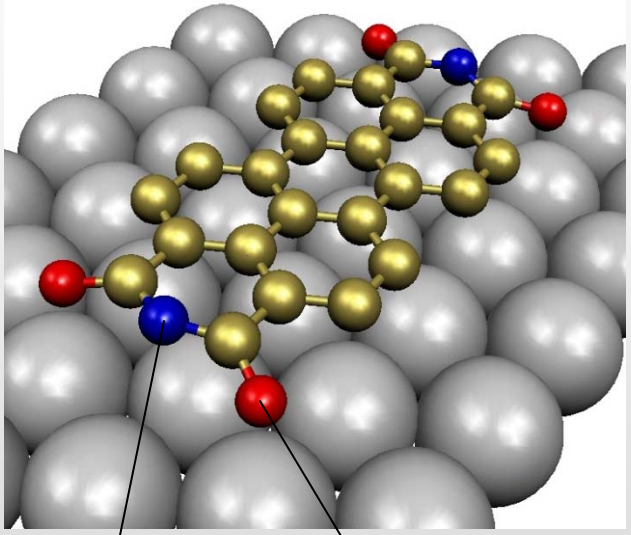

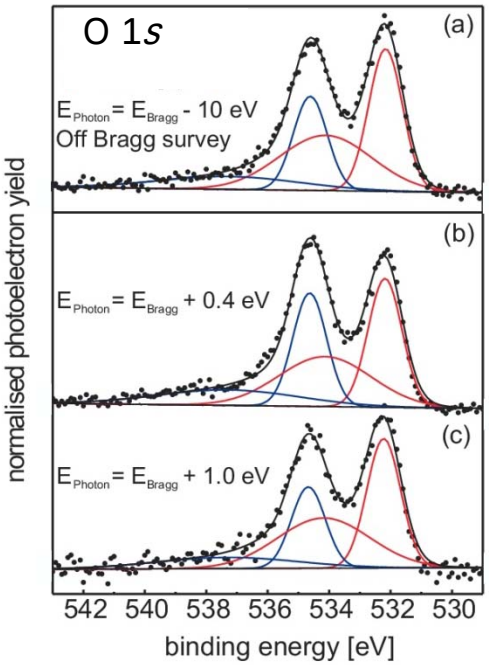

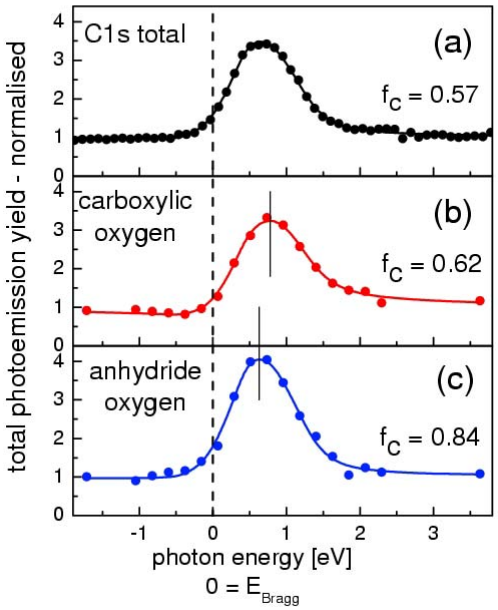

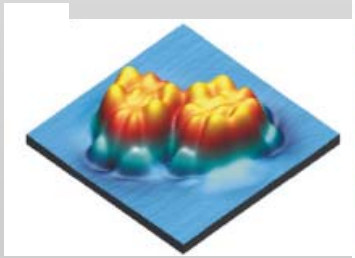

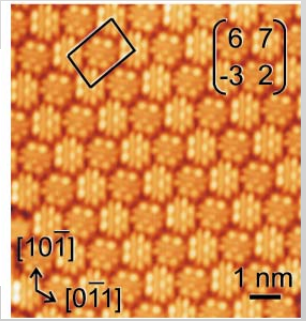

Hauschild et al., ESRF Highlights 2005

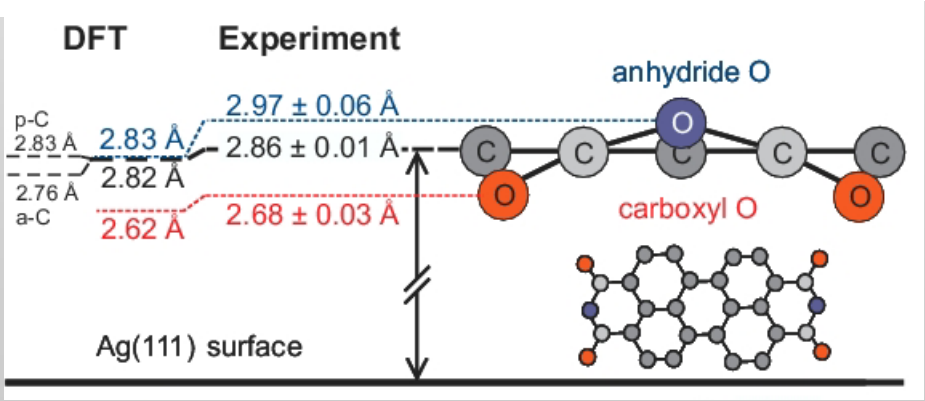

Combine core-level shift detection with XSW
α-Sn/Ge(111) surface: Dynamic fluctuations at room temperature

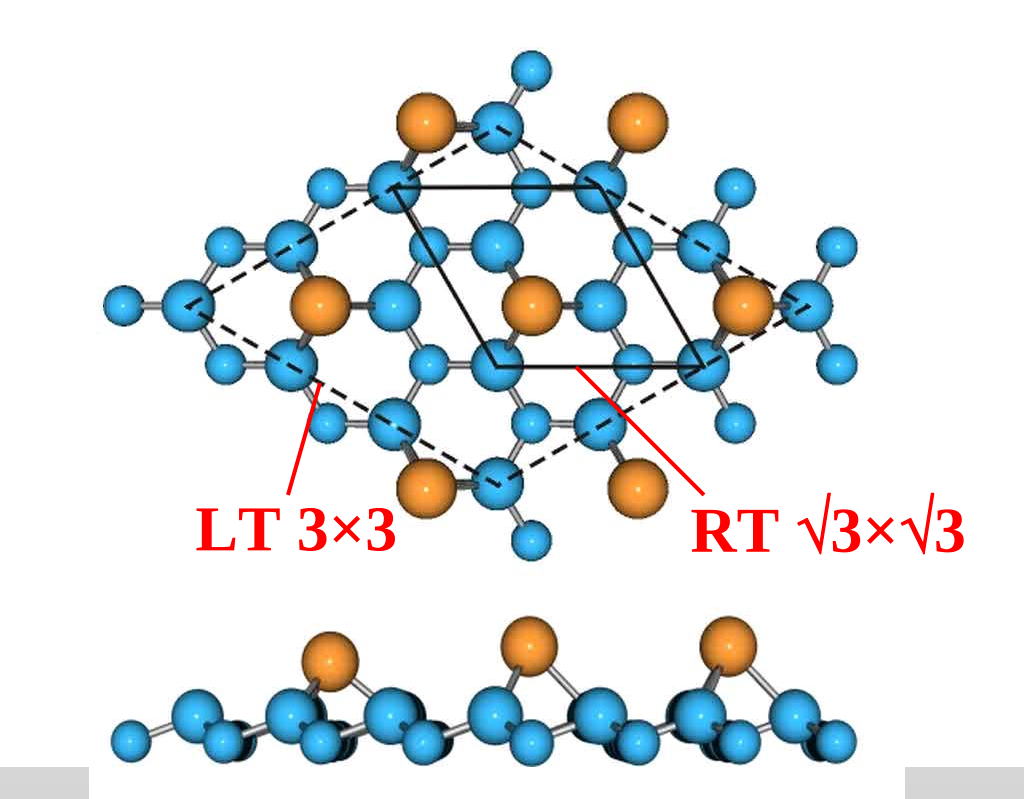

α-Sn/Ge(111) surface

- A seemingly simple structure: **T_4 site** adsorption of 1/3 ML of Sn adatoms
- **Electron counting of dangling bonds per surface unit cell**
  ⇒ Metallic and unstable ??
- RT √3×√3 ↔ LT 3×3 phase transition at ~ 200 K
- Main question: **structure of the RT phase**

* *Fluctuation model: J. Avila et al., PRL* ***82****, 442 (1999).*

* *Calculations: G. Ballabio et al., PRL 89, 126803 (2002)*

RT Sn/Ge(111) probed by **hard x-ray photoelectron spectroscopy**

(hν = 2510 eV with ΔE ~ 500 meV)

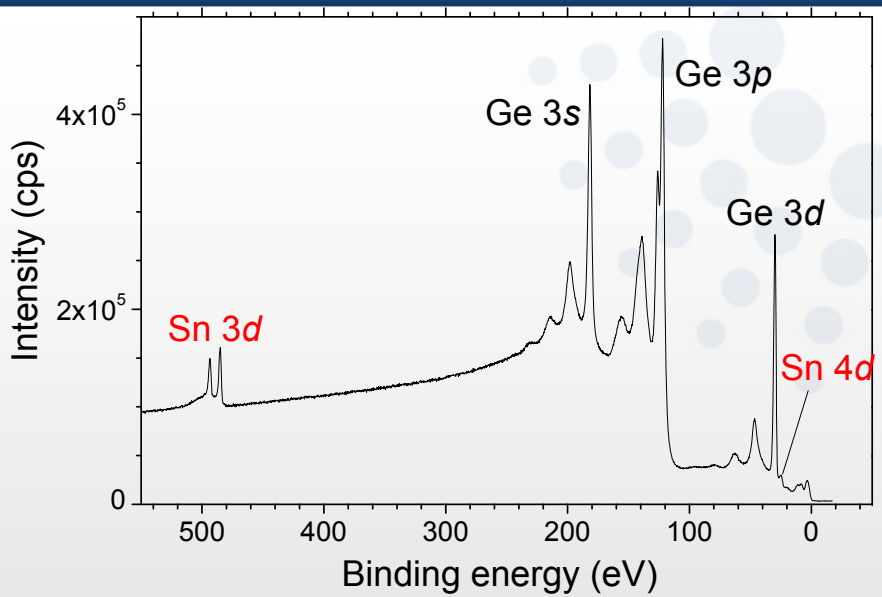

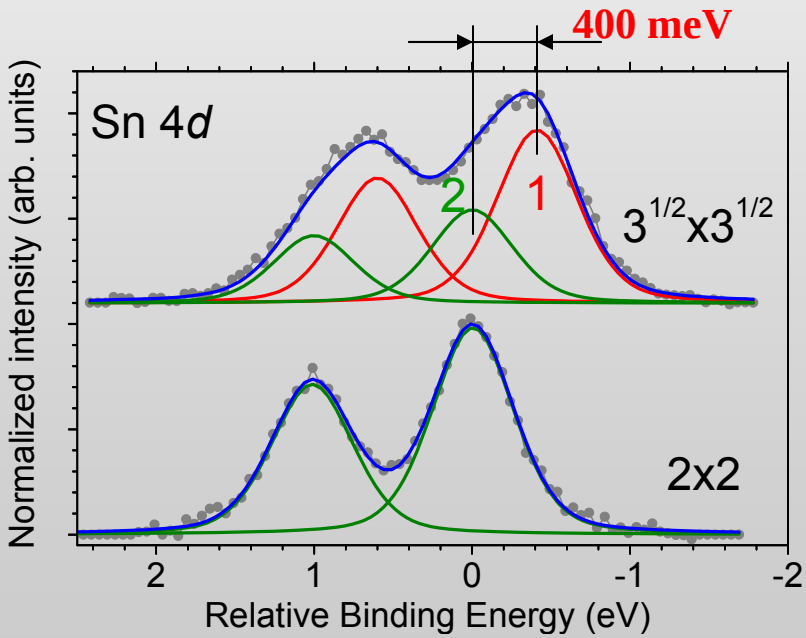

$\sqrt{3}\times\sqrt{3}$ (1/3 ML)

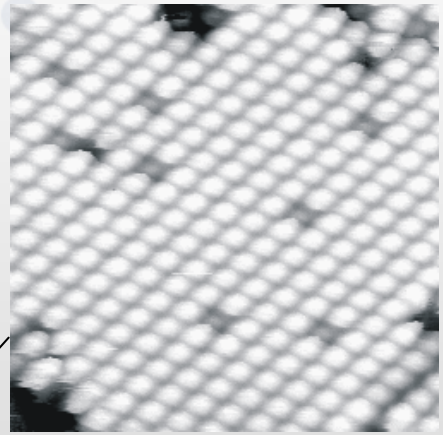

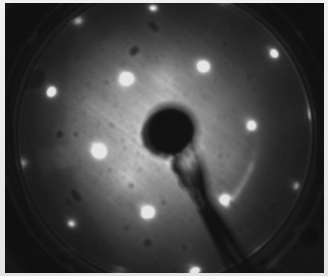

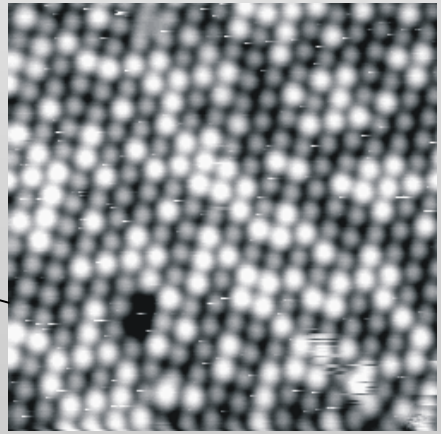

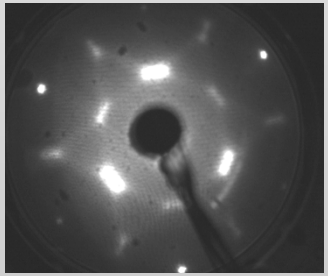

2x2 (< 0.2 ML)

RT Sn 4*d* core-level spectra modulated by Ge(111) XSW

(normalized to the peak height)

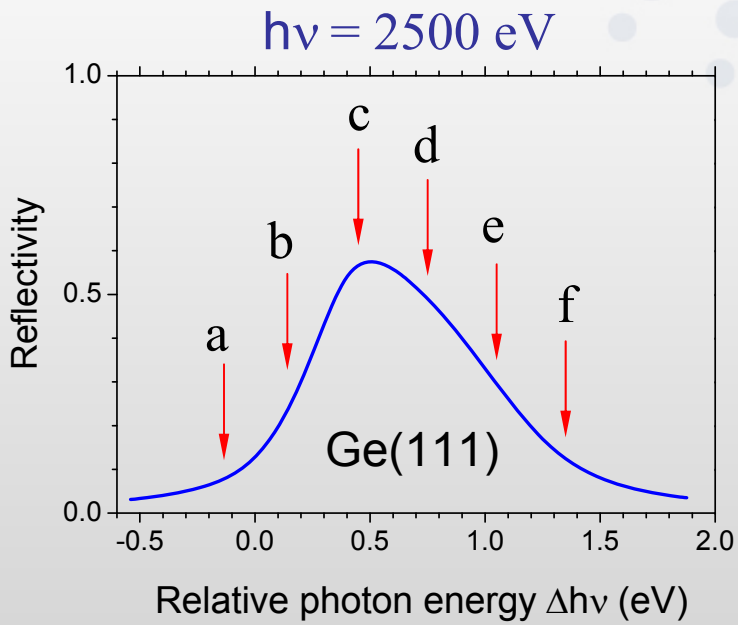

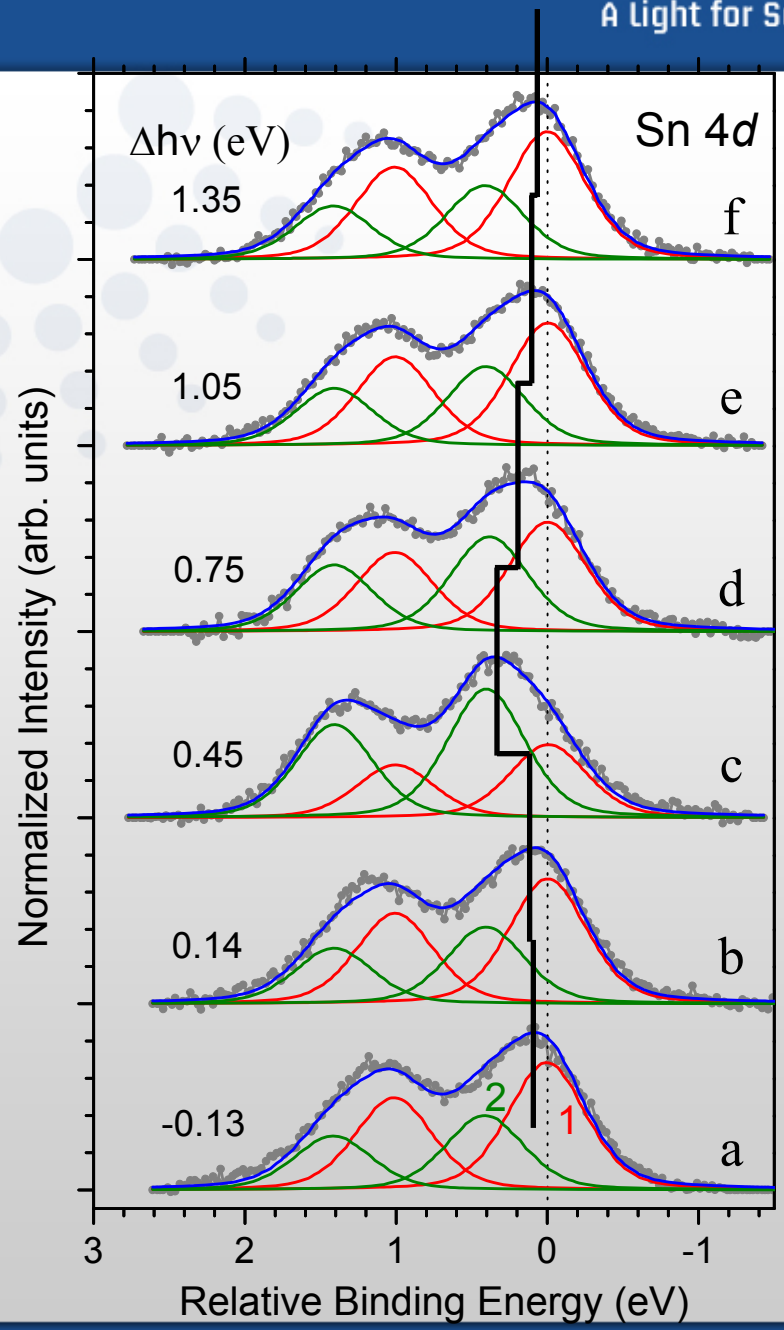

Intensity ratio I_1/I_2 varies with hν

⇒ Sn 1 & 2 are modulated differently

⇒ **2 Sn sites**

RT investigation of Sn 3*d* core-level shift

E = 2.5 keV ± ΔE

Core hole lifetime width of Sn 3d ~ 400 meV

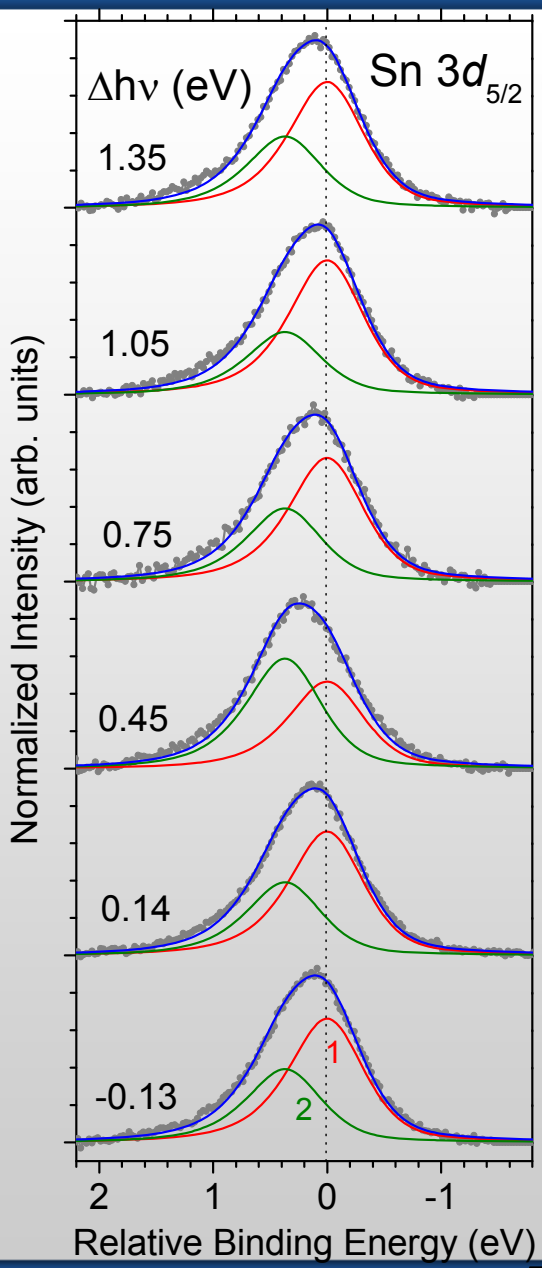

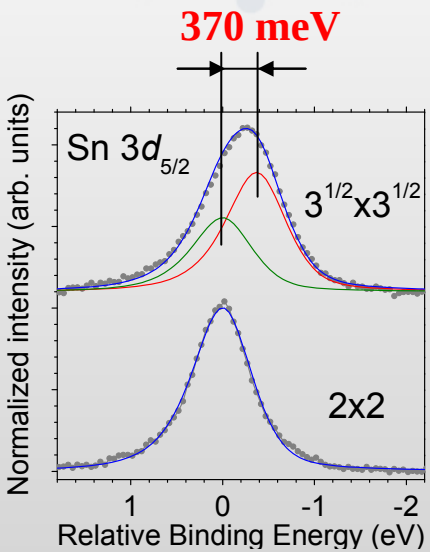

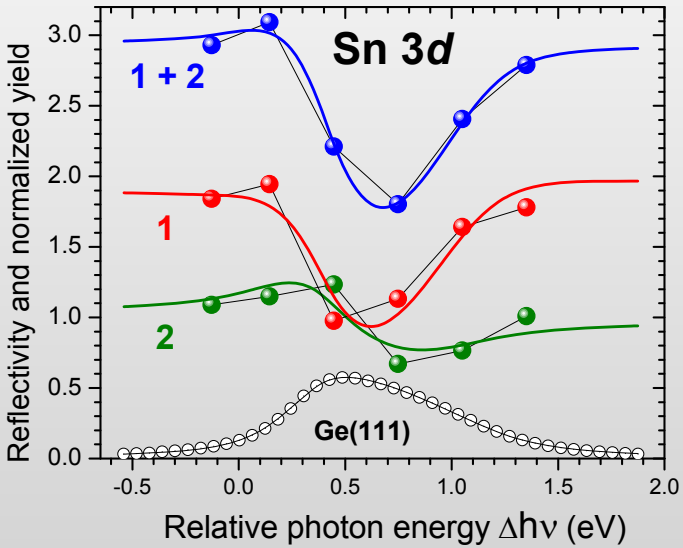

<= Ge(111) XSW modulated spectra

Ge(111):Sn RT √3x√3 – XSW/XPS Analysis

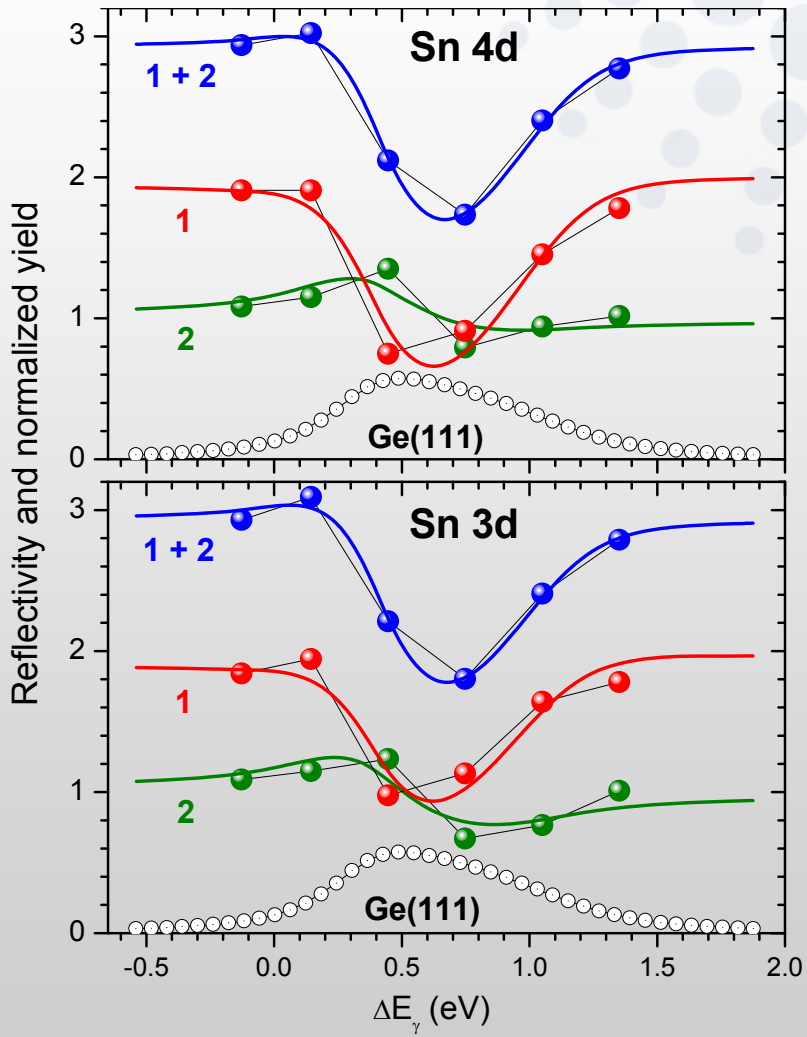

	Comp	f_{111}	P_{111}	I_1/I_2	h (Å)	Δh (Å)
3*d*	1+2	*0.66*	*0.78*	***1.92***	*2.55*	***0.23***
	1	*0.75*	*0.80*		*2.61*	
	2	*0.52*	*0.73*		*2.38*	
4*d*	1+2	*0.68*	*0.79*	***1.96***	*2.58*	***0.23***
	1	*0.86*	*0.80*		*2.61*	
	2	*0.40*	*0.73*		*2.38*	

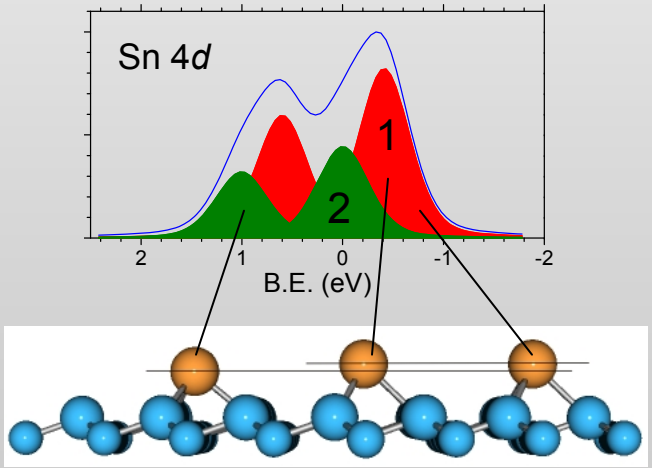

T.L. Lee, B.C.C. Cowie, S. Warren, J. Zegenhagen, Phys. Rev. Lett. **96,** 046103 (2006)

What does XSW measure ?

Yield: $Y(\theta) \propto 1 + R(\theta) + 2\sqrt{R(\theta)} \cdot f_H \cdot \cos[\nu(\theta) - 2\pi P_H]$

e.g. Fluorescence

Reflectivity — Coherent fraction — Phase difference — Coherent position

Element-specific "structure factor": $\mathbf{G_H} = \int_{V_{uc}} \rho(\mathbf{r}) \cdot e^{2\pi i \mathbf{H}\cdot\mathbf{r}} d\mathbf{r} = f_H \cdot e^{2\pi i P_H}$

Normalized **atomic** distribution, element specific

X-ray Standing Wave Analysis of Bismuth Implanted in Si(110)
N. Hertel, G. Materlik and J. Zegenhagen
Z. Phys. B Condensed Matter 58, 199 – 204(1985).

XSW

- *measures directly phases of "structure factors"* ↔ *phase problem in diffraction*
- *is element and chemical-state specific and sensitive to low-Z elements*
- *does not require long-range order*
- *offers high spatial resolution*

- *requires good-quality crystals* → *backscattering geometry*
- *provides only folded structural information (no info on length scales* $> a_{substrate}$*)*

Imaging complex atomic structures with X-ray Standing Waves

X-ray Standing Wave Imaging

The Growth of the First Monolayer $YBa_2Cu_3O_{7-\delta}$ on $SrTiO_3(001)$

STM

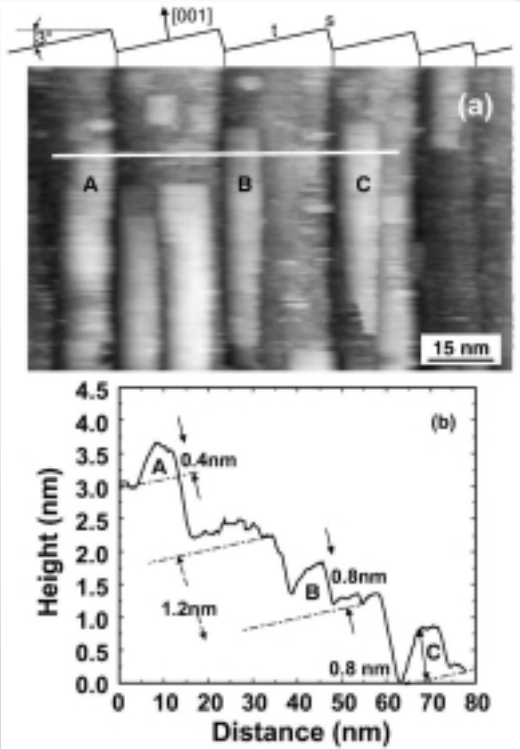

*T. Haage, J. Zegenhagen, H. –U Habermeier, M. Cardona, PRL **80**, 4225 (1998)*

$SrTiO_3$
perovskite

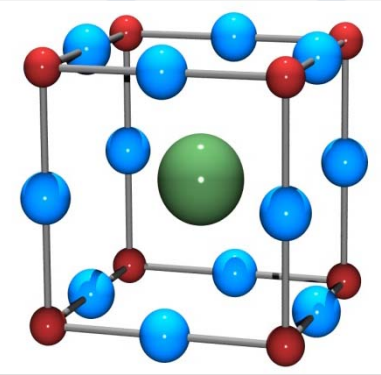

Sr
O
Ti

a = 0.391 nm

$YBa_2Cu_3O_{7-\delta}$
Superconductor. T_c = 90 K

Ba
Y
Ba

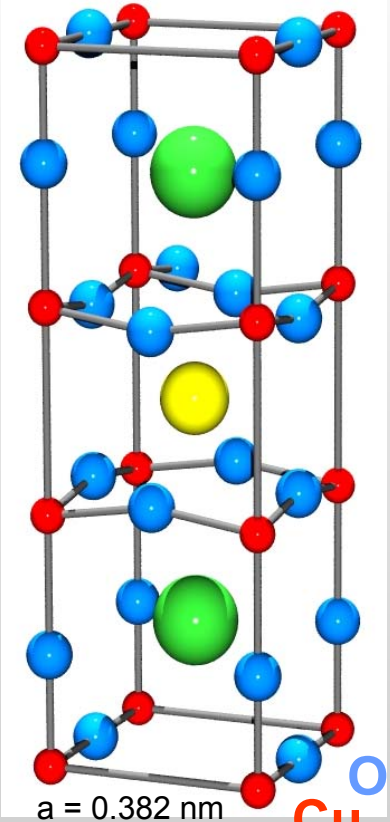

c =1.168 nm

O
Cu

a = 0.382 nm
b = 0.389 nm

Experimental

- sample: 0.5 ±0.1 ML $YBa_2Cu_3O_{7-\delta}$ deposited on $SrTiO_3(001)$

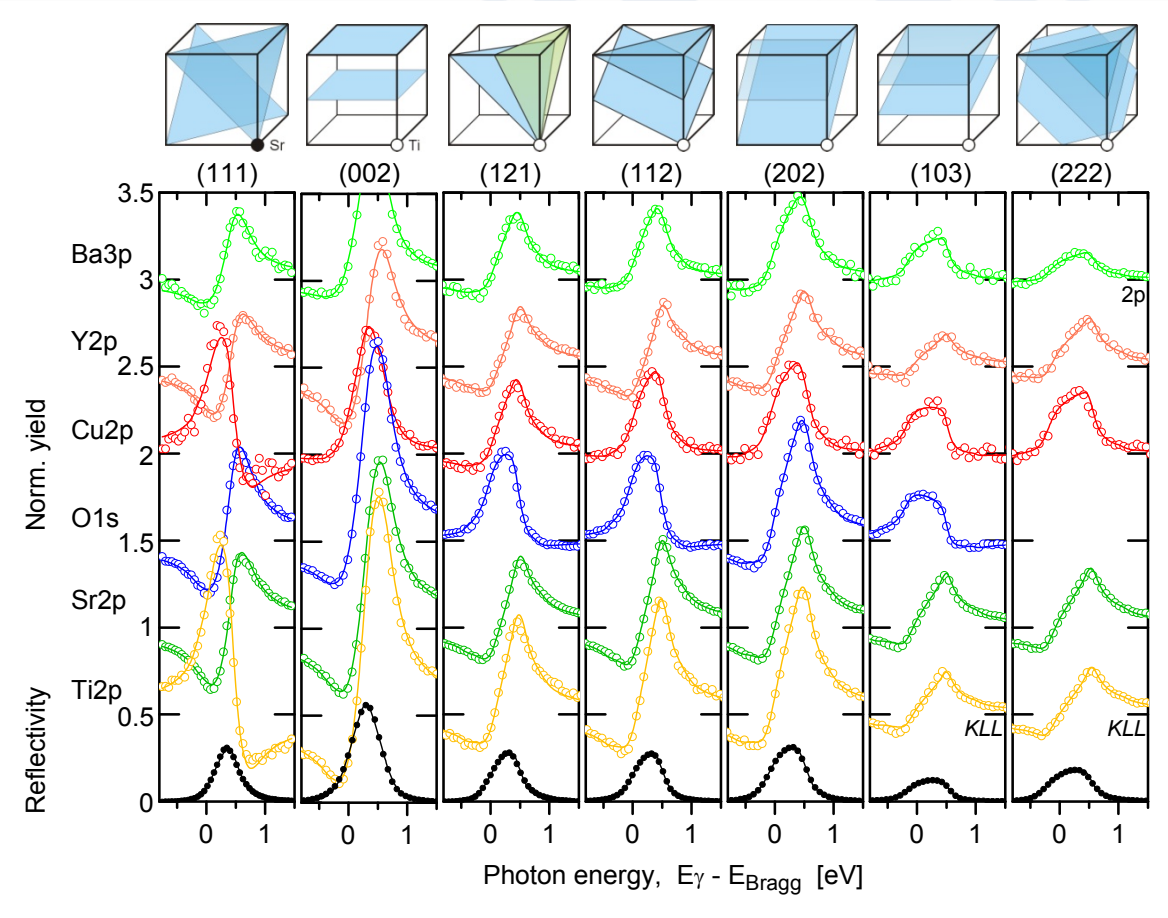

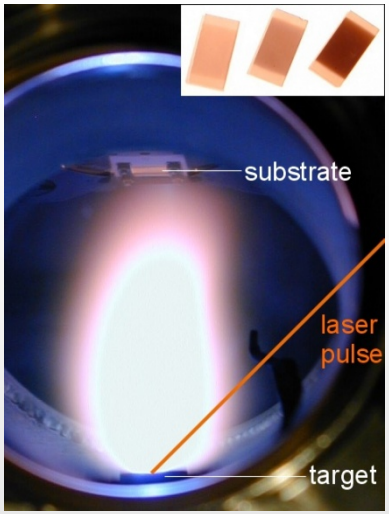

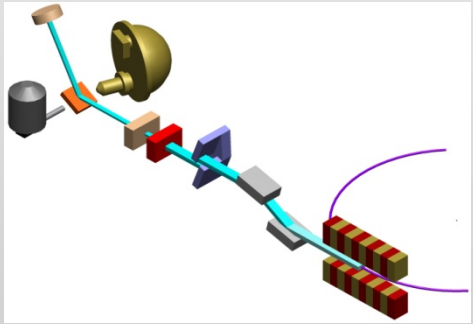

- real space image reconstruction: $\rho(\mathbf{r}) = 1 + 2\sum_{\mathbf{H}} f_{\mathbf{H}} \cdot \cos[2\pi i(P_{\mathbf{H}} - \mathbf{H}\cdot\mathbf{r})]$

3D reconstructed images

0.5 ML $YBa_2Cu_3O_{7-\delta}$

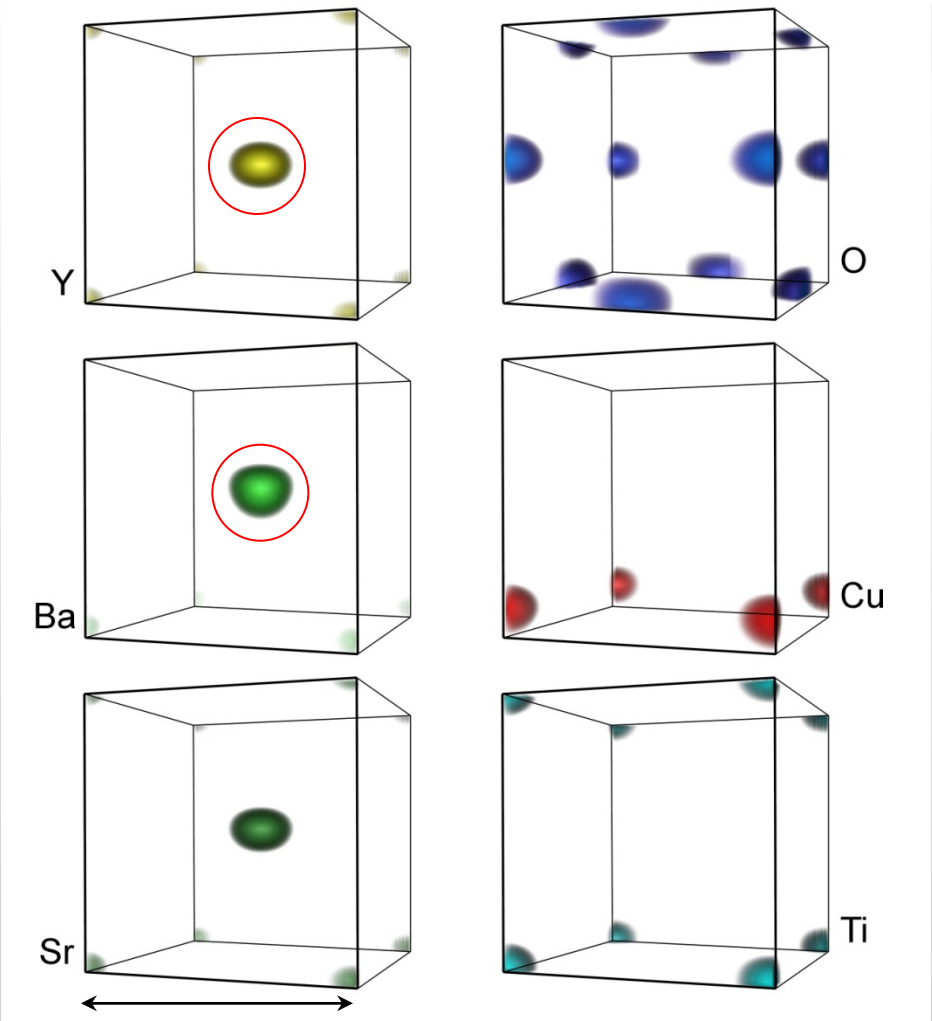

~ 4 Å

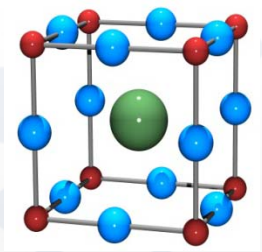

Perovskite structure

$YBa_2Cu_3O_{7-\delta}$

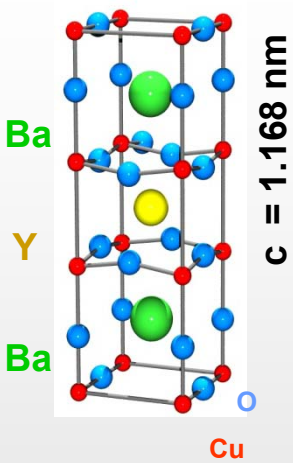

- perovskite structure
- oxygen visible
- 2 distinct layer spacings
- Y and Ba occupy different sites

projections into the $SrTiO_3$ unit cell

Site specific photoelectron emission

Site-specific decomposition of the $SrTiO_3$ valence band

Valence Yield excited by

1) ... a single X-ray beam:

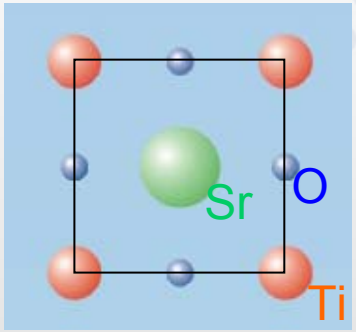

$SrTiO_3$

2) ... an XSW field:

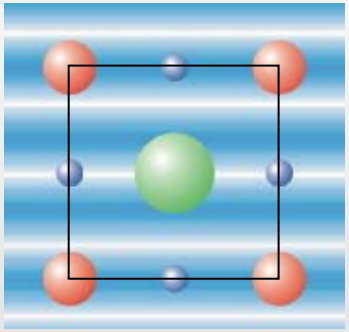

$$Y_{VB}(E_B) = \left\{ \sum_{j = Sr, Ti, O_3} Y_j(E_B) \right\}$$

$$Y_{VB}(E_B, E_\gamma) = \sum_{j = Sr, Ti, O_3} I_j(E_\gamma) \cdot Y_j(E_B)$$

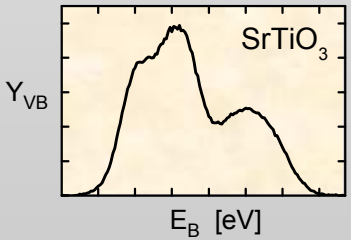

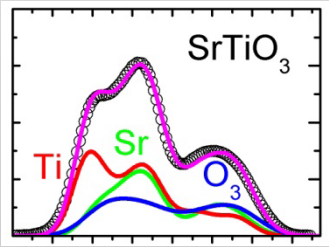

XSW modulated valence band spectra of $SrTiO_3$

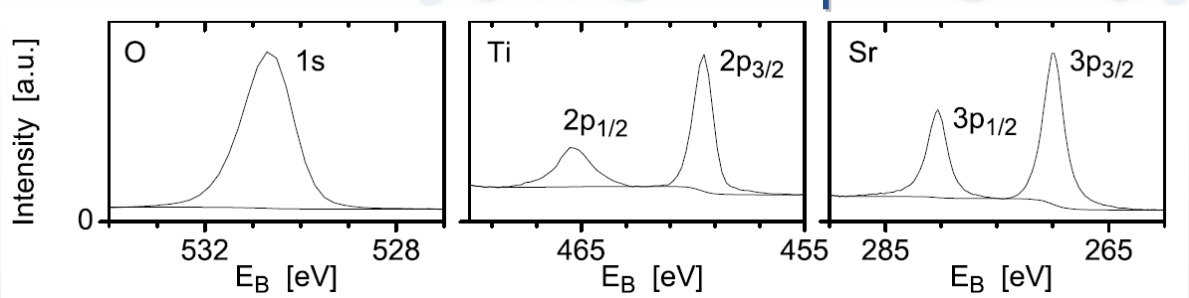

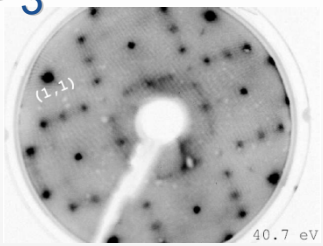

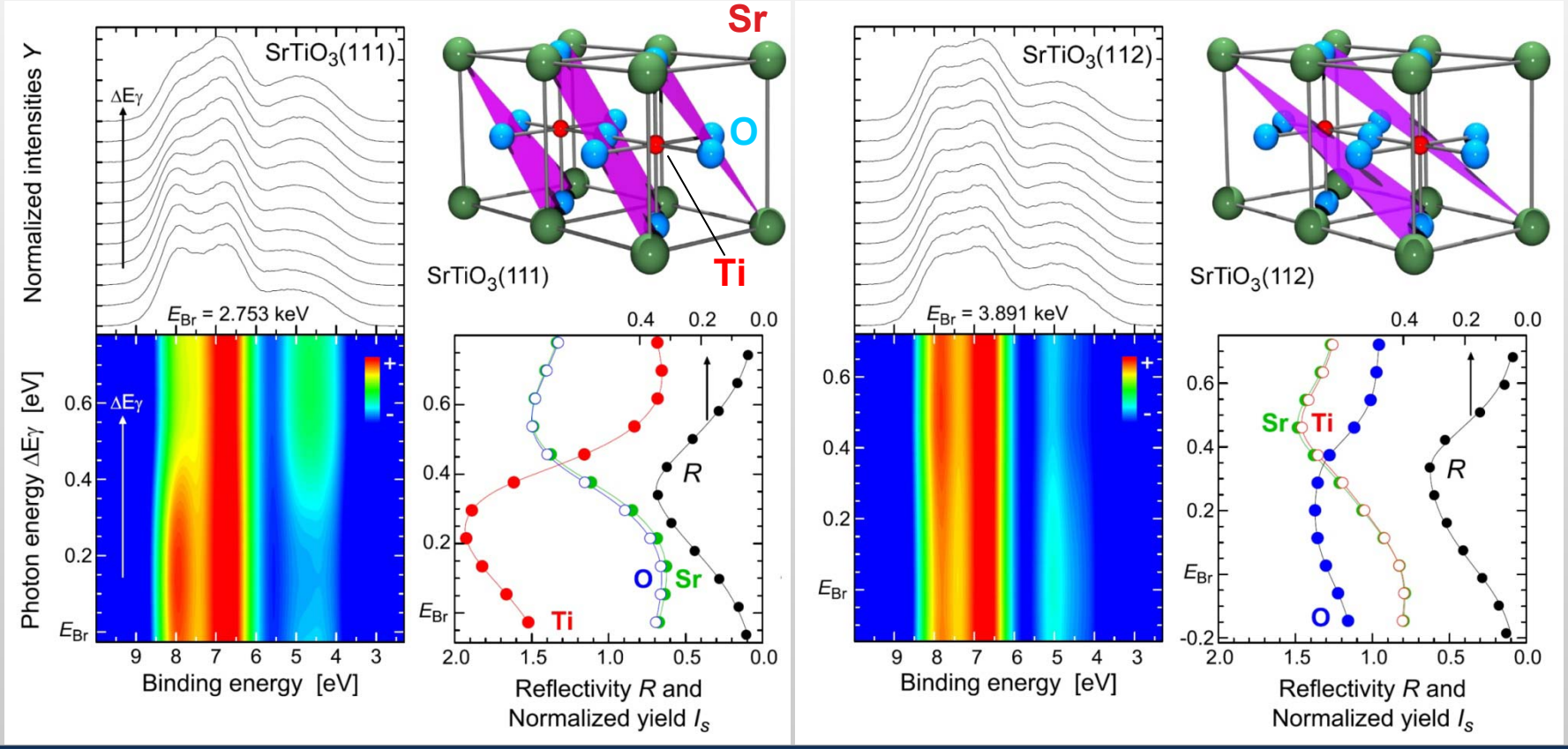

Site-specific valence electronic structure of $SrTiO_3$

$SrTiO_3(111)$ $SrTiO_3(112)$

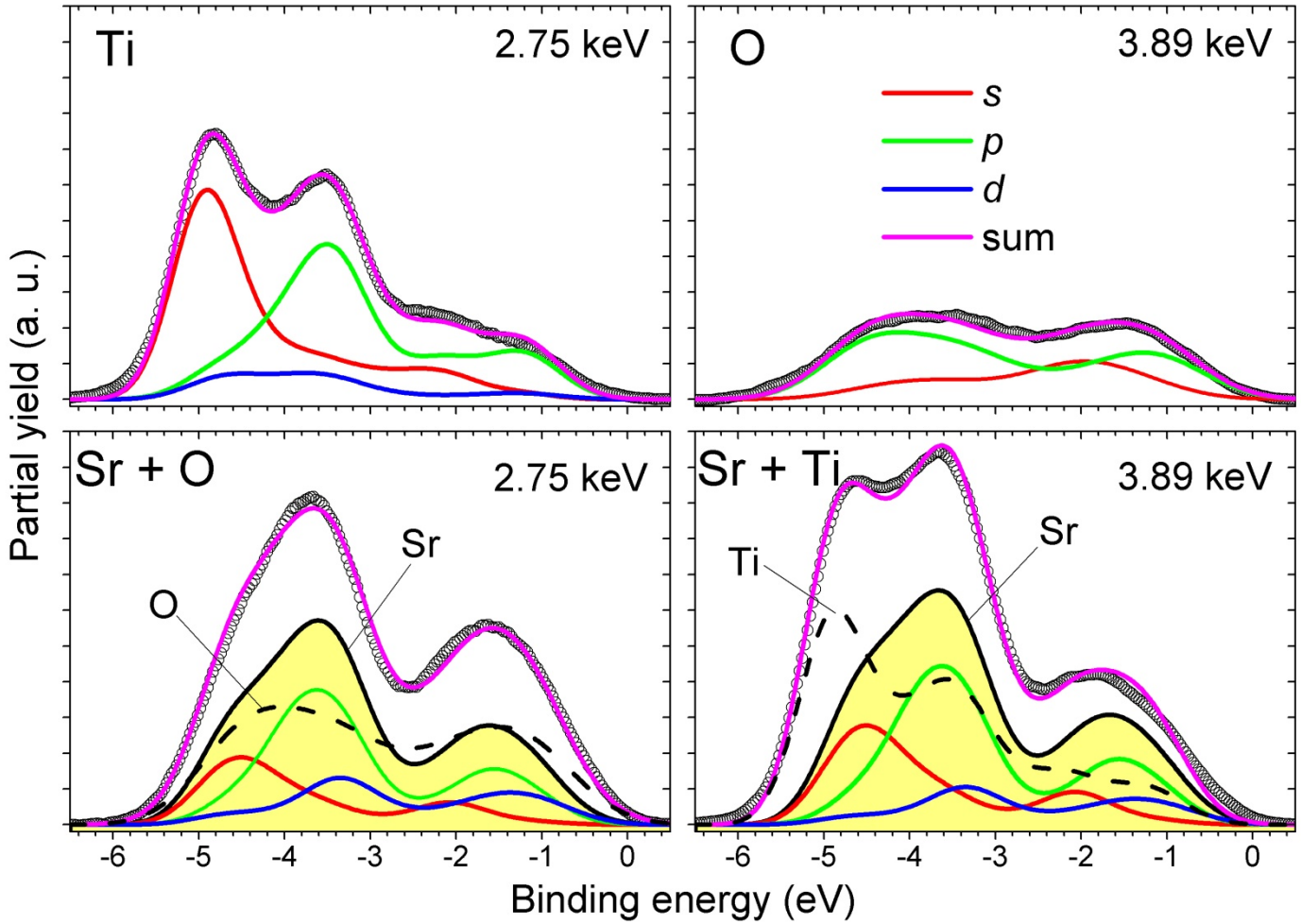

Direct decomposition of STO valence band

Compare Ti and O partial yields with theoretical lpDOS

Determine Sr partial yields: Assuming

$$R_{solid} = c\,R_{atom}$$

where

$$R = \frac{\sigma(3.89\ \text{keV})}{\sigma(2.75\ \text{keV})}$$

Valence band decomposition of $SrTi0_3$ by XSW

And comparison with ab-initio LDA calculations

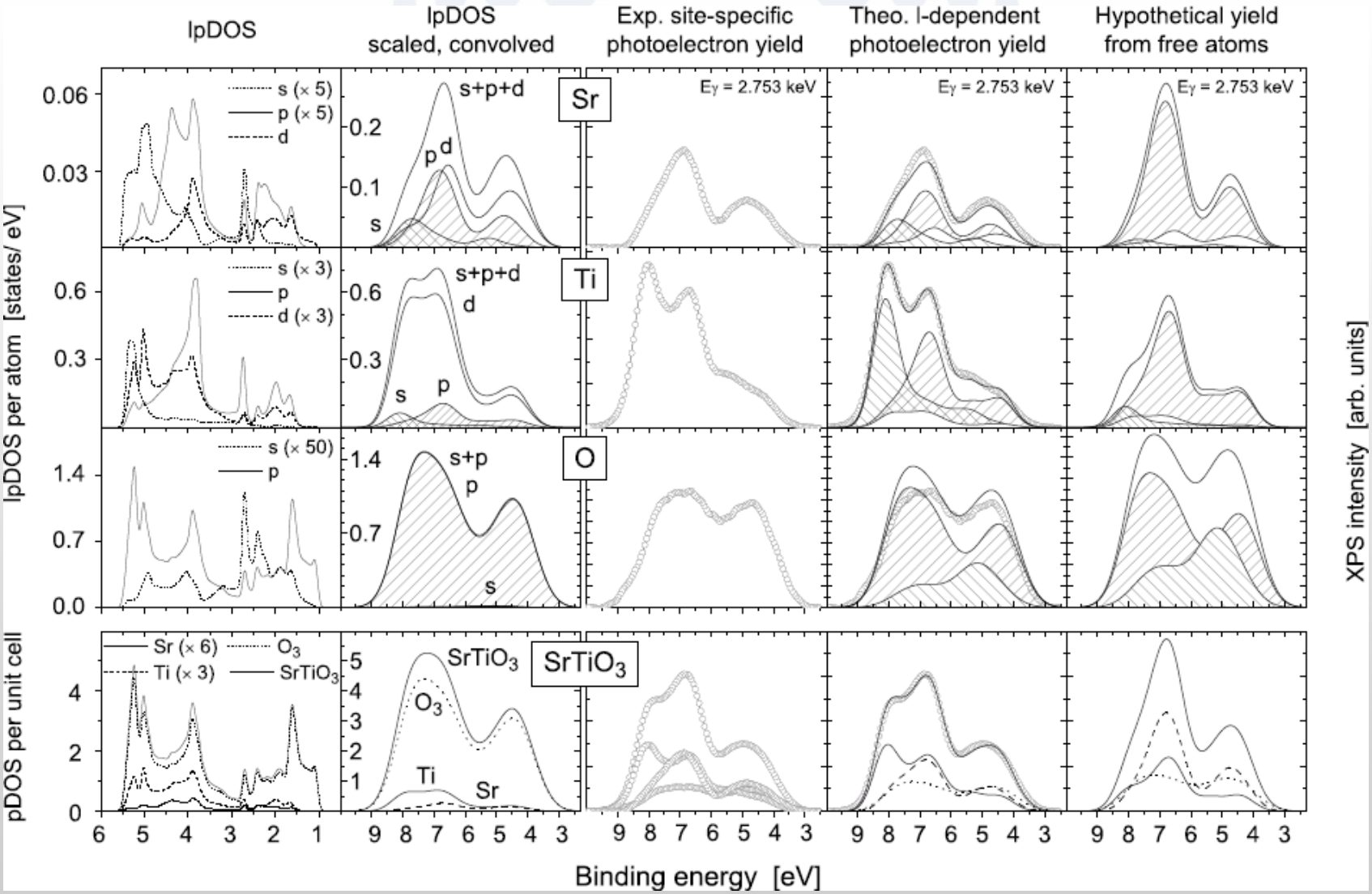

Beyond dipole approximation: Influence on differential cross section

$$I_{SC} = I_{OB}[1 + S_R R + S_I 2\sqrt{R} F^{\mathbf{H}} \cos(\varphi - 2\pi P^{\mathbf{H}} + \psi)$$

Because of backward/forward asymmetry the photoelectron yield excited by the incident and the reflected wave is no longer equivalent in the photoelectron emission

As a consequence, the "yield function" Is modified by three parameters

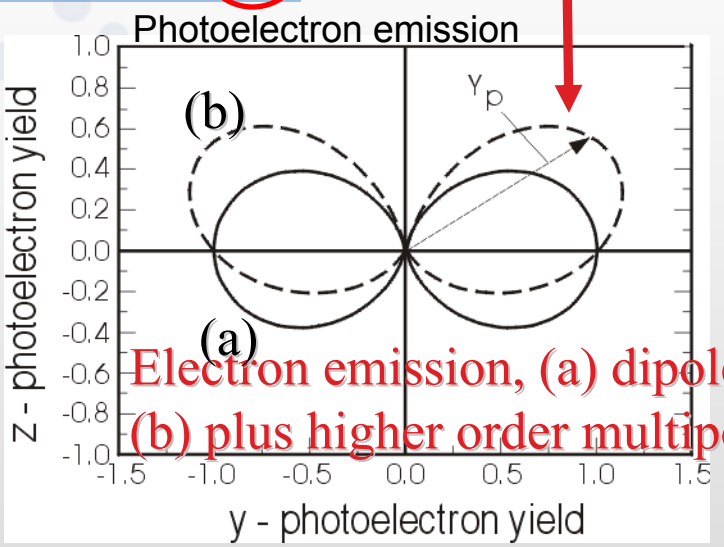

Electron emission, (a) dipole, (b) plus higher order multipole

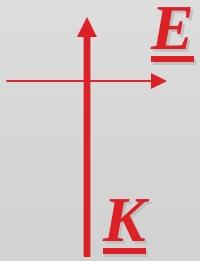

Multipole contributions affect different orbitals differently

$$I_{SC} = I_{OB}[1 + S_R R + S_I 2\sqrt{R} F^{\mathbf{H}} \cos(\varphi - 2\pi P^{\mathbf{H}} + \psi)$$

XSW/PE from $SrTiO_3$

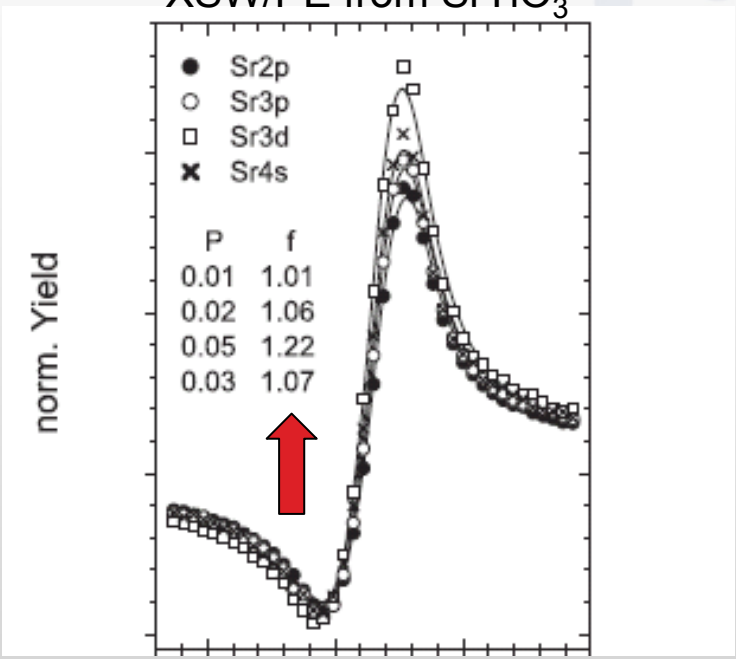

$f = S_I * F^H$

Photoelectron emission

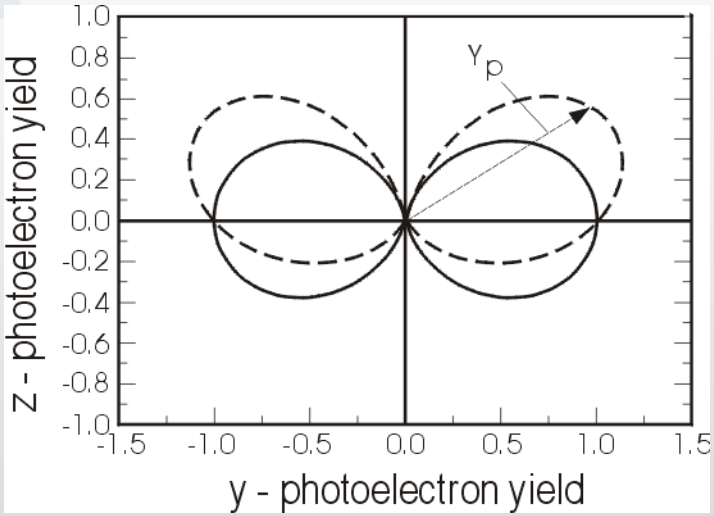

PE emission quadrupole parameters published by:
M. B. Trzhaskovskaya, V. K. Nikulin, V. I. Nefedov, and V. G. Yarzhemsky, At. Data Nucl. Data Tables 92, 245 (2006).

I. Vartanyants et al. / Nuclear Instruments and Methods in Physics Research A 547 (2005) 196–207

New HAXPES set-up at ID32

New HAXPES set-up at ID32

ID32 – Experimental Hutch 2 – EH2

UHV/XPS set-up 2, PHOIBOS 225, 15 keV

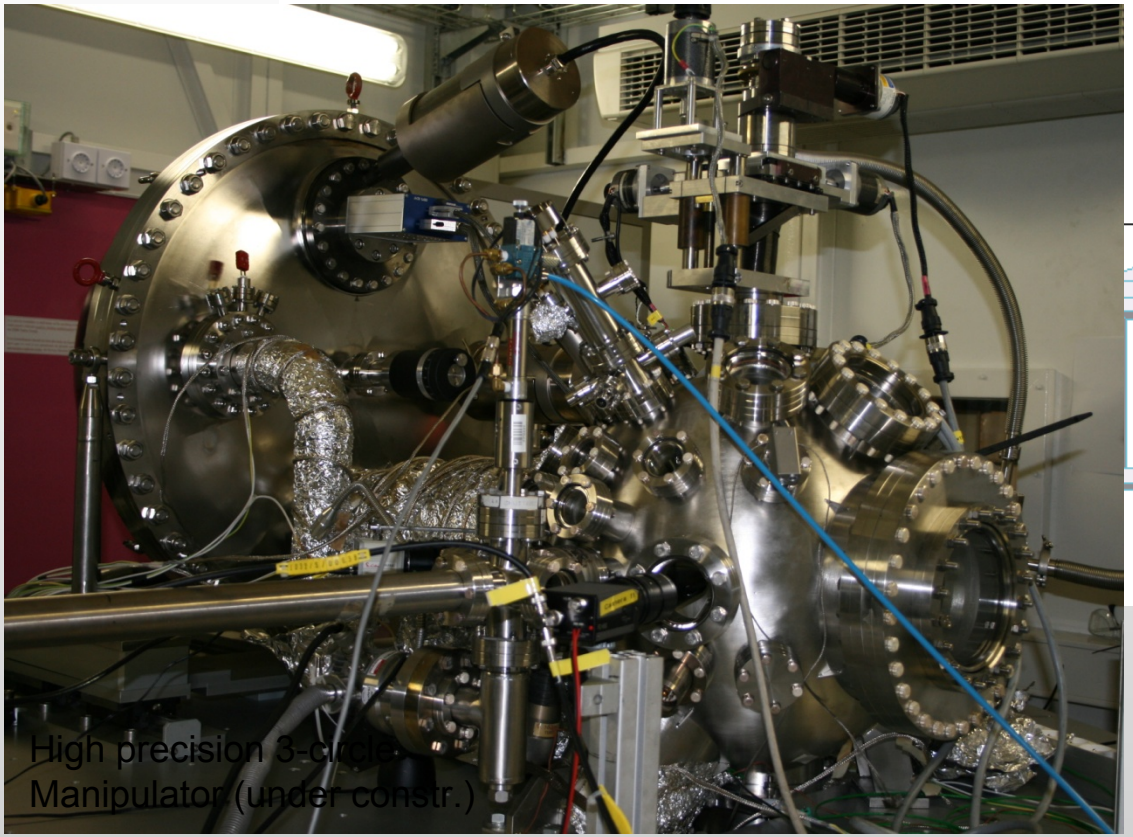

UHV/XPS set-up 1; PHI, 4.8 keV

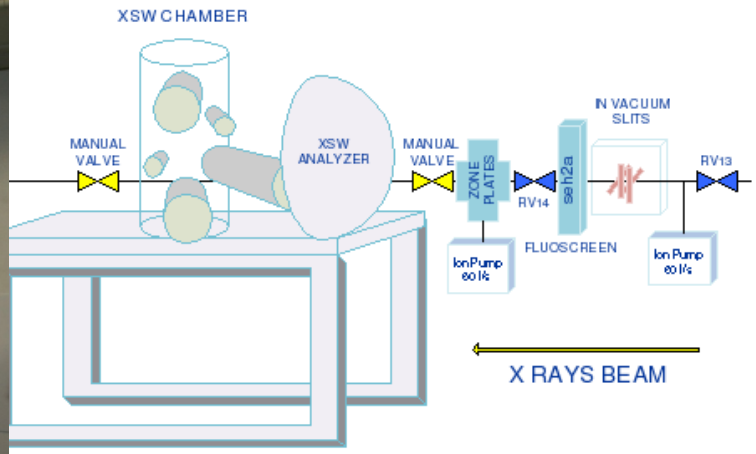

ID32 - Optics Hutch 2 – OH2

Mirror, three stripes: SiO_2, Ni, Pd

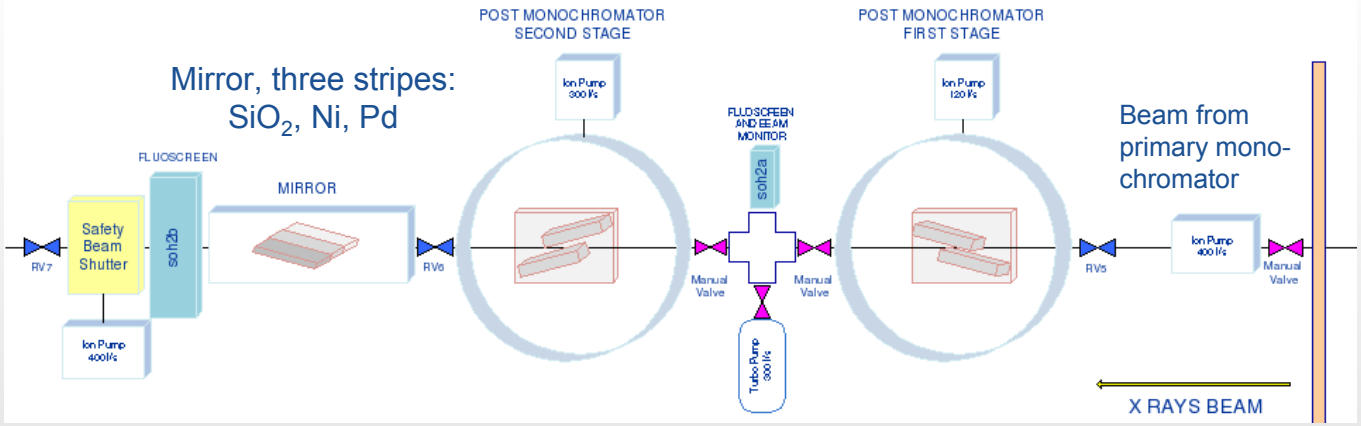

Beam from primary mono-chromator

Postmono modes

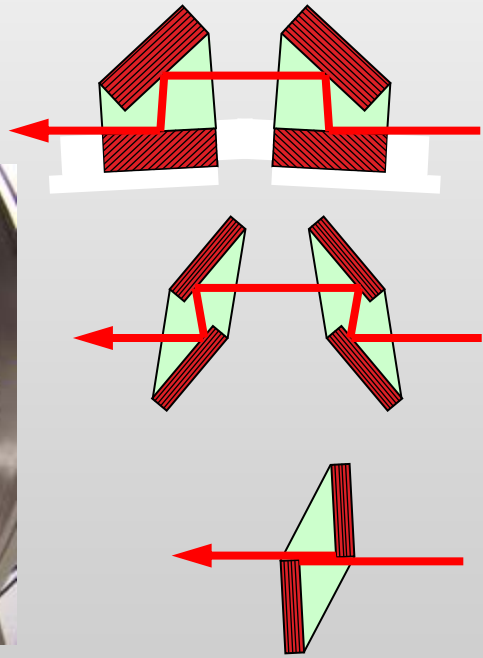

High resolution secondary monochromators in UHV ; view inside

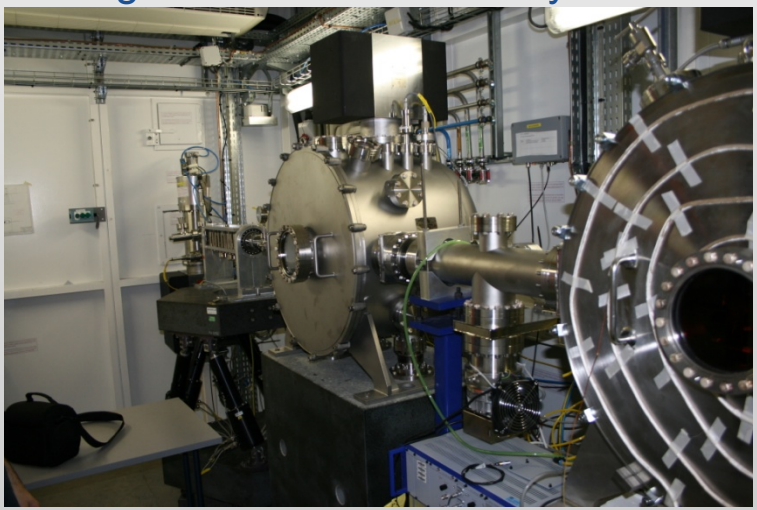

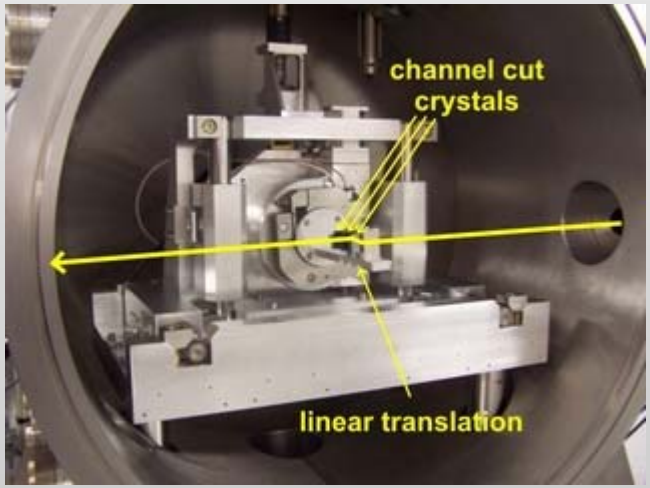

Up to five sets of channel cut crystals can be selected

SPECS PHOIBOS 225 HV

(delivered & installed spring/summer 2008)

- For electron energies up to 15 keV
- Different modes of operation
  (UPS, XPS and HAXPES)
- Ultra high energy resolution in
  UPS < 1meV
  HAXPES <15 meV
- Angular Mapping ($\Delta\Theta < 0.1°$)
- Detectors: 2D delay-line detector (or CCD)
- Spatial resolution < 50 µm
- Large working distance (53 mm)

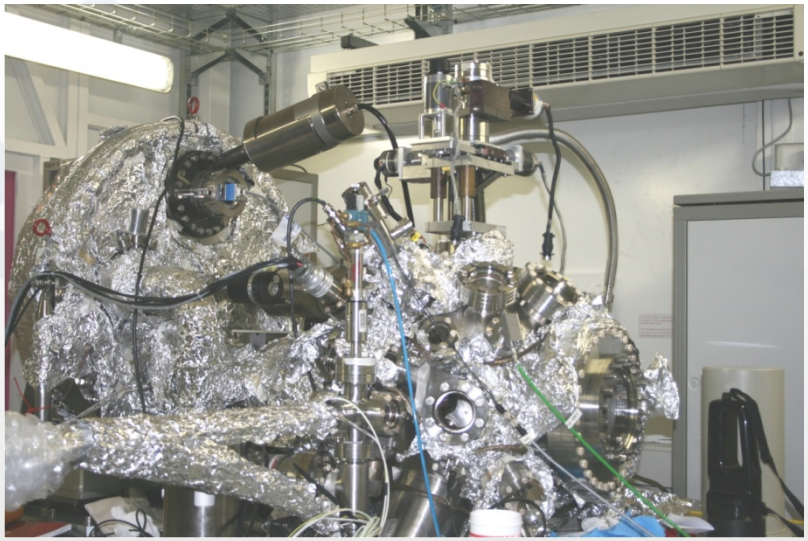

Cu 2p resonant XPS of $La_{2-x}Sr_xCuO_4$ at Cu K edge

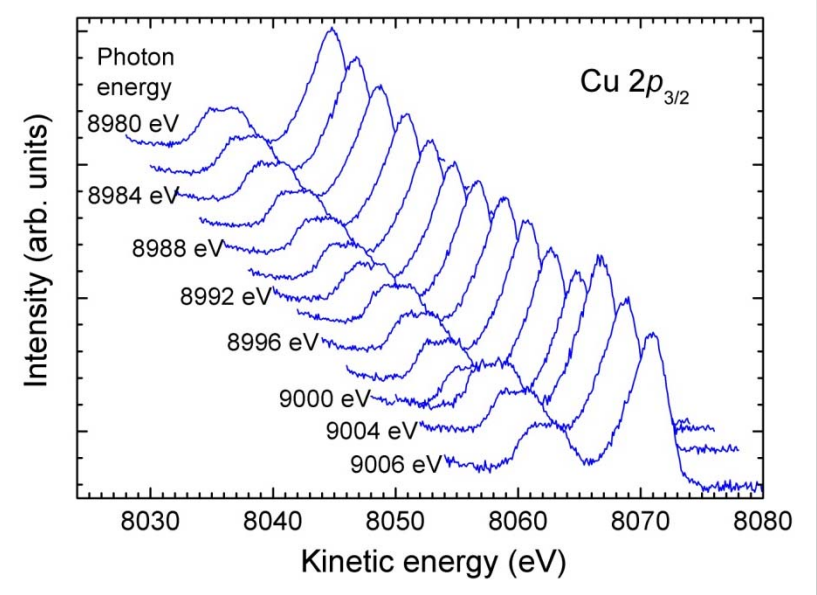

Used for a few studies:

HAXPES studies of metal oxide and nitride stacks related to CMOS technology (STMicroelectronics, Crolles)

Conclusion

- Combination of XSW with HAXPES very powerful (chemical shift, ...);
  higher order XSW measurements (Fourier components) require higher PE KE
- $SrTiO_3$ XSW/XPS VB yield agrees well with theory, some cross sections influenced by solid state, also: peak broadening (*see poster by Sebastian Thiess*)
- XSW imaging: $YBa_2Cu_3O_{7-\delta}$ nucleates on $SrTiO_3$ as perovskite: Investigating complex oxide interfaces with XSW and XPS/HAXPES very valuable since the structure can be unfolded element specific (including oxygen)
- In interpreting XSW/PES data: Be aware of multipole contributions
- New HAXPES set-up at ID32 slowly approaching specifications (15 keV < 50 meV)
  → *Latest results : see poster by Blanka Detlefs*

Acknowledgement: Tien-Lin Lee, *now at DIAMOND Light Source*
→ talk SISA beamline at DIAMOND, Friday
Francois Bottin, *CEA/DAM Ile-de-France*
Sebastian Thiess, *now at HASYLAB/DESY*
Helena Isern, *ESRF/ID32&ID03*
Bruce Cowie, *now at Australian Light Source*
Lucien Petit, *ESRF/ID32&ID03*
Lionel Andre, *ESRF/ID32*
Blanka Detlefs, Yanyu Mi, Jerome Roy, *ESRF/ID32*
BMBF ($$$)

Thank you for your attention

END

Katsushika Hokusai (1760-1849):
The Great Wave Off Kanagawa
(Fugaku sanjurokkei: Kanagawaoki namiura).
from the **Thirty-Six Views of Mount Fuji** (circa 1826-33).

XSW/VB analysis of SrTiO3

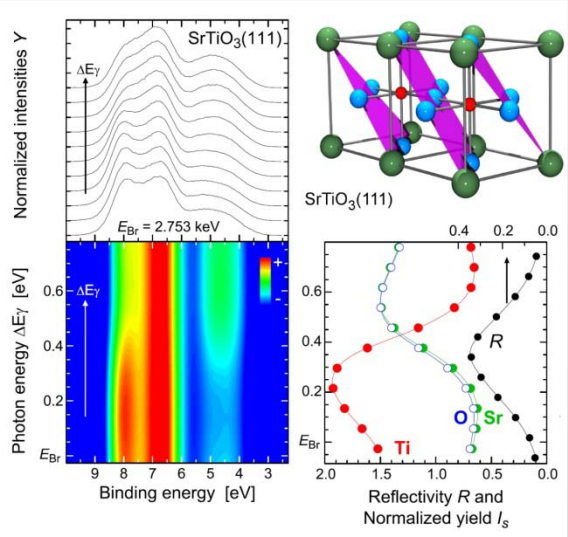

✓ Theoretical lpDOS shows good agreement with the site-specific partial yields determined by XSW for the $SrTiO_3$ valence band.

✓ The XSW-decomposed spectra allow clear identification of hybridization between the metal and oxygen derived states.

✓ Comparison with the previous VB-XSW study on TiO_2 (Woicik *et al.*) indicates the effects of distortion of the $(TiO_6)^{8-}$ octahedron on the valence band.

✓ The photoionization cross sections of the metal s states are found to be much larger in the solid than the values for the corresponding atomic states.

Sebastian Thiess, Tien-Lin Lee, François Bottin, and Jörg Zegenhagen, in preparation for PRL

Inelastic scattering: Photoexcitation and dipole approximation

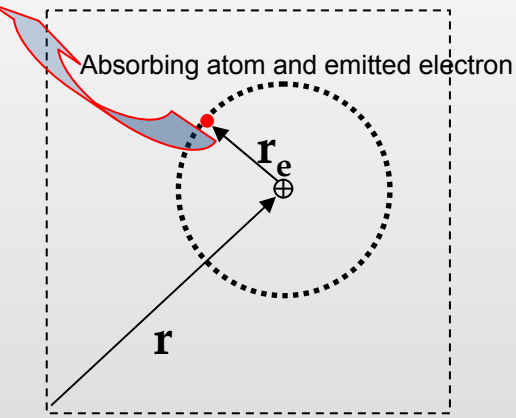

Reference frame, e.g., crystal unit cell

$$\mathbf{M_{fi}} \propto \int d^3 r_e \psi_f^* \mathbf{A}\mathbf{p}\psi_\mathbf{i}$$

$$\mathbf{A} = \mathbf{A_0} e^{-2\pi i \mathbf{K_0 r}} (\vec{E}_0 + \vec{E}_H \sqrt{R} e^{i\varphi} e^{-2\pi i \mathbf{Hr}})$$

is no function of the electron position $\mathbf{r_e}$, thus,

$$\mathbf{M_{fi}} \propto \mathbf{A} \int d^3 r_e \psi_f^* \mathbf{p}\psi_\mathbf{i}, \mathbf{p} = (\hbar/i)\nabla$$

and in case that the polarization vectors are coplanar

$$\sigma_D \propto |\mathbf{M_{fi}}|^2 \propto |\mathbf{A}|^2 \propto \left|1 + R + \sqrt{R} e^{i(\varphi - 2\pi \mathbf{Hr})}\right|^2$$

Cross section σ_D

With the cross section σ also the electron yield is proportional To $|\mathbf{A}|^2$, i.e., to the intensity of the wavefield

Ge(111):Sn RT √3x√3 – XSW/XPS Analysis

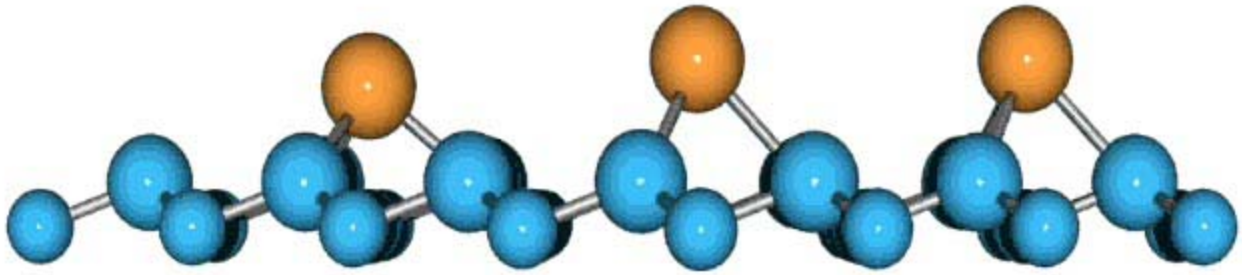

A seemingly simple structure: **T4 site** adsorption of 1/3 ML of Sn adatoms, but atoms occupy two different heights and flip fast and thus appear to be equivalent e.g. in STM images

Phase versus amplitude (XRD vs XSW)

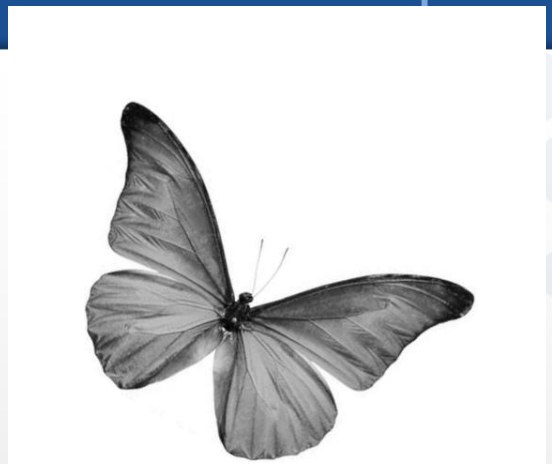

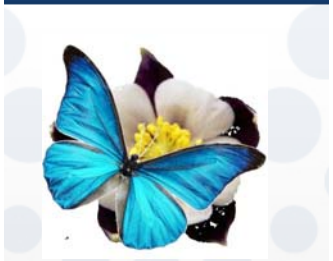

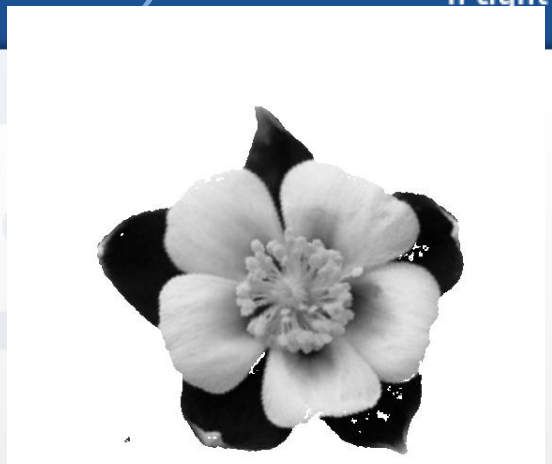

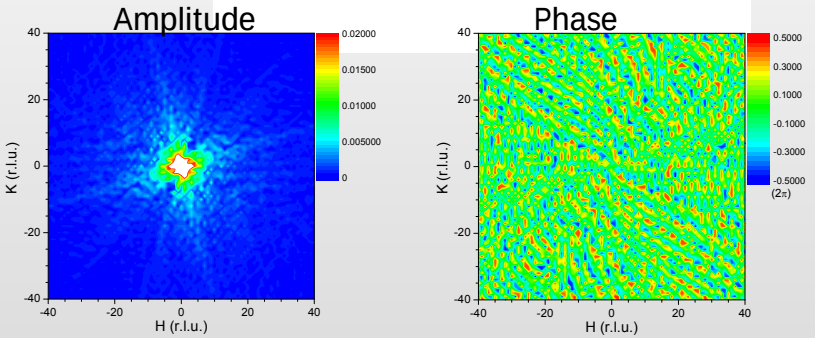

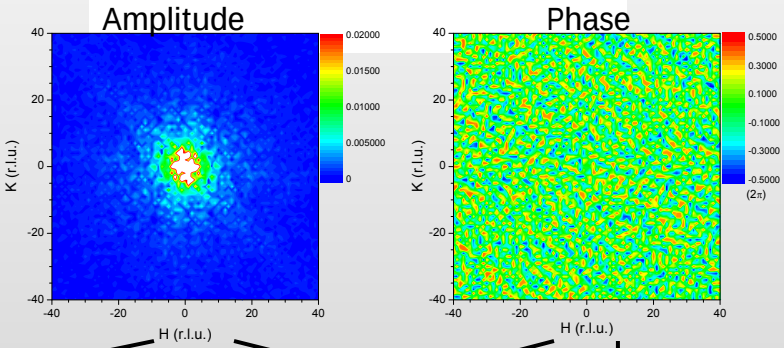

Electronic density of states of $SrTiO_3$ - *ab initio* LDA calculations (Francois Bottin)

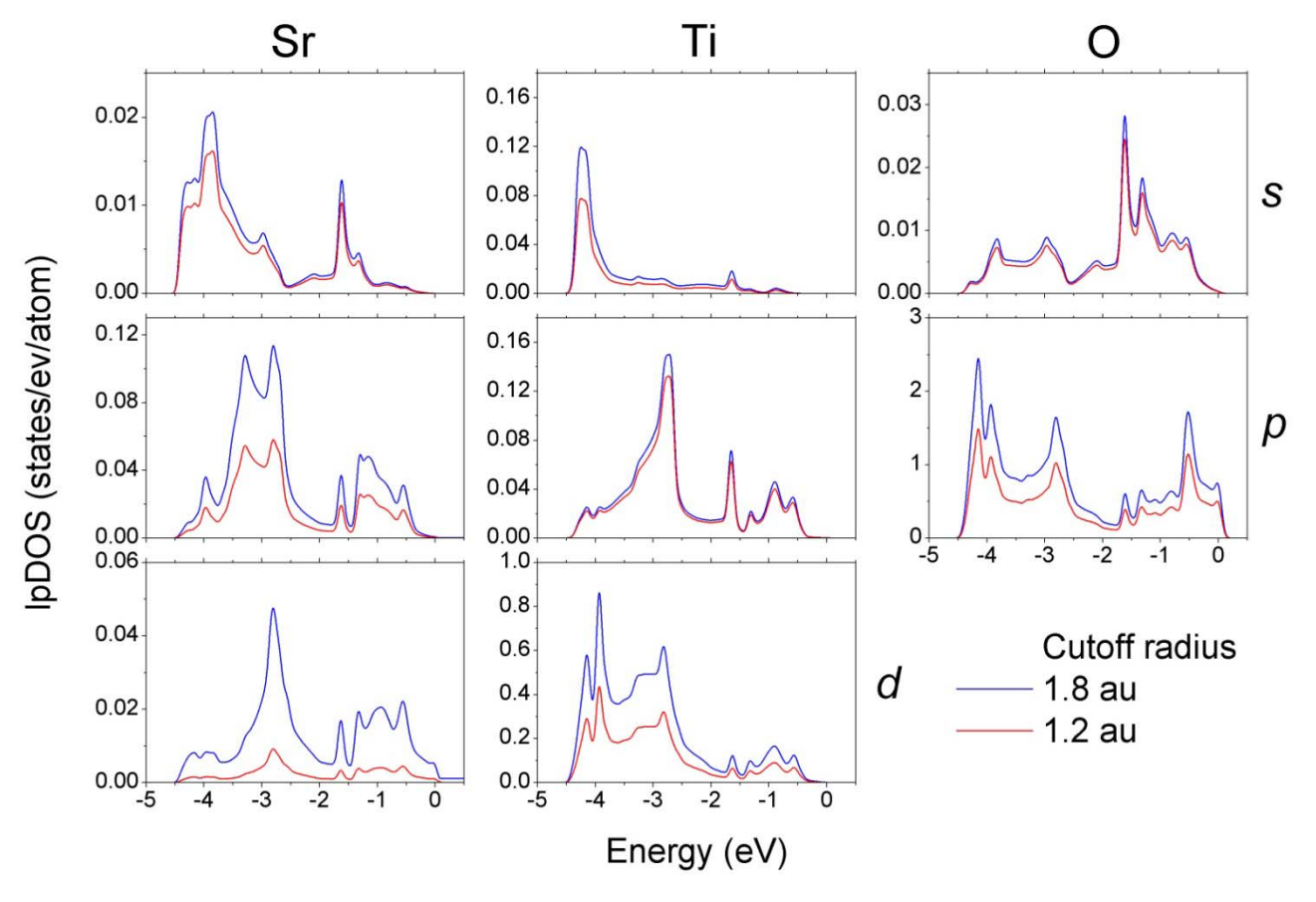

(after convolution with a Gaussian of 100 meV FWHM)

- ✓ Troullier-Martins Pseudopotentials
- ✓ Electronic configurations:

  Sr: $4s^2 4p^6 5s^2$
  Ti: $3s^2 3p^6 4s^0 3d^4$
  O: $2s^2 2p^4$
  (+ 14 unoccupied states)
- ✓ Plane-wave cutoff energy: 140 Ry
- ✓ Monkhorst-Pack mesh: 6 × 6 × 6

Solid-state vs atomic cross sections for valence electrons

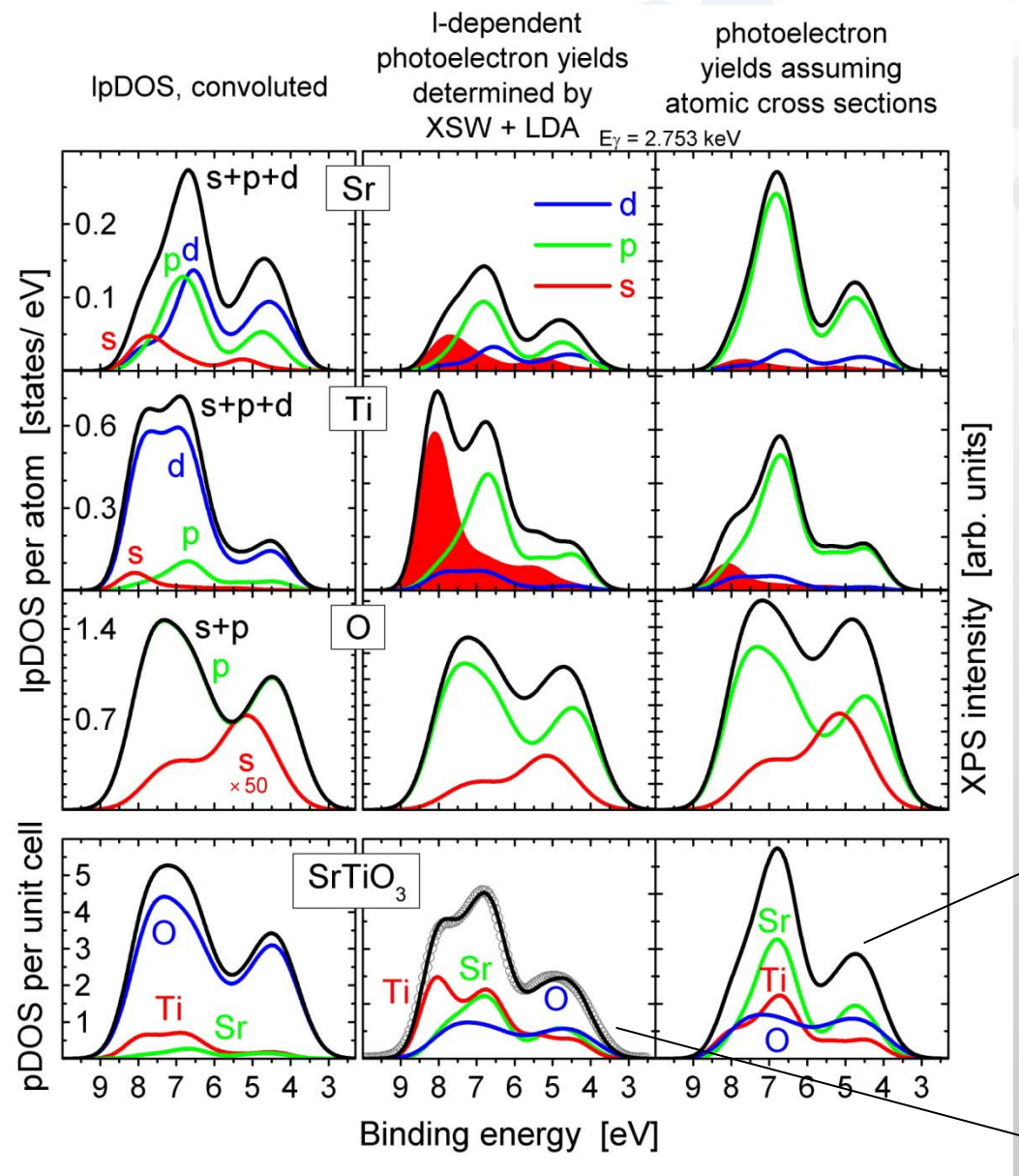

For each sub-shell,

$$Y^{at}(E_b) = \rho(E_b)\ (1+\beta^{at})\ n\ \sigma^{at}$$

lpDOS

Atomic dipole parameter

Number of valence electrons
(from the lpDOS)

Atomic cross section per electron

Trzhaskovskaya et al., at. data nucl. data tab. ***77****, 97 (2001)*

720 barn

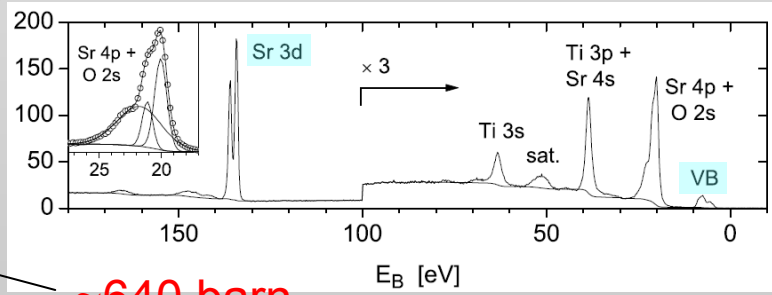

~640 barn

Comparison with molecular-orbital energy levels of octahedral symmetry

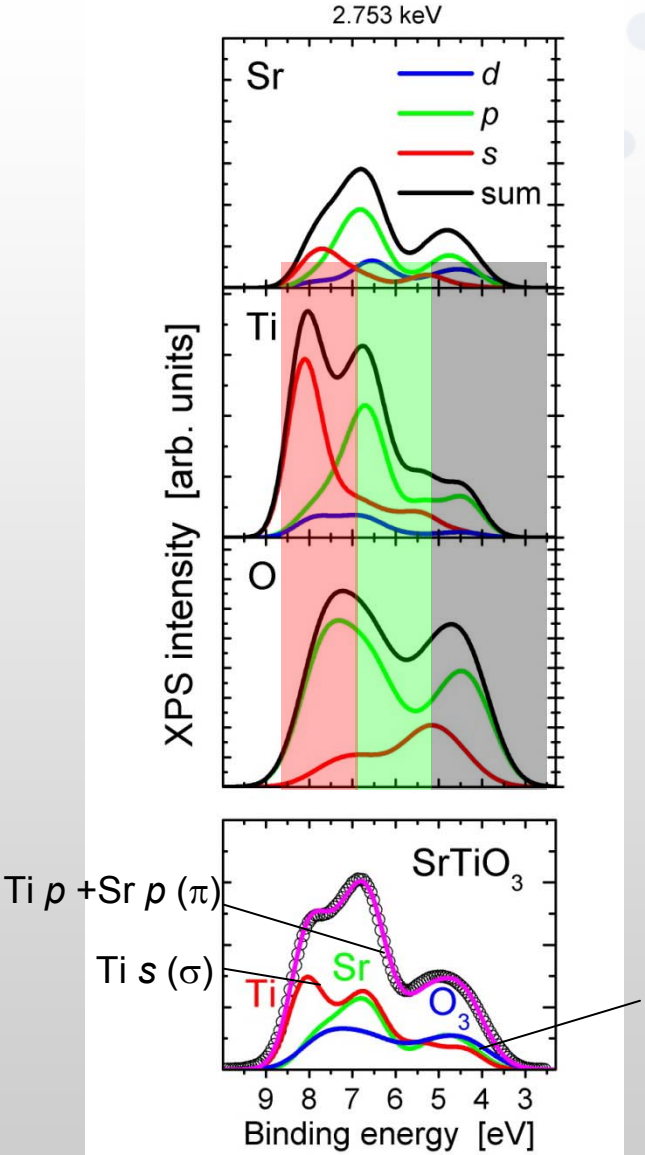

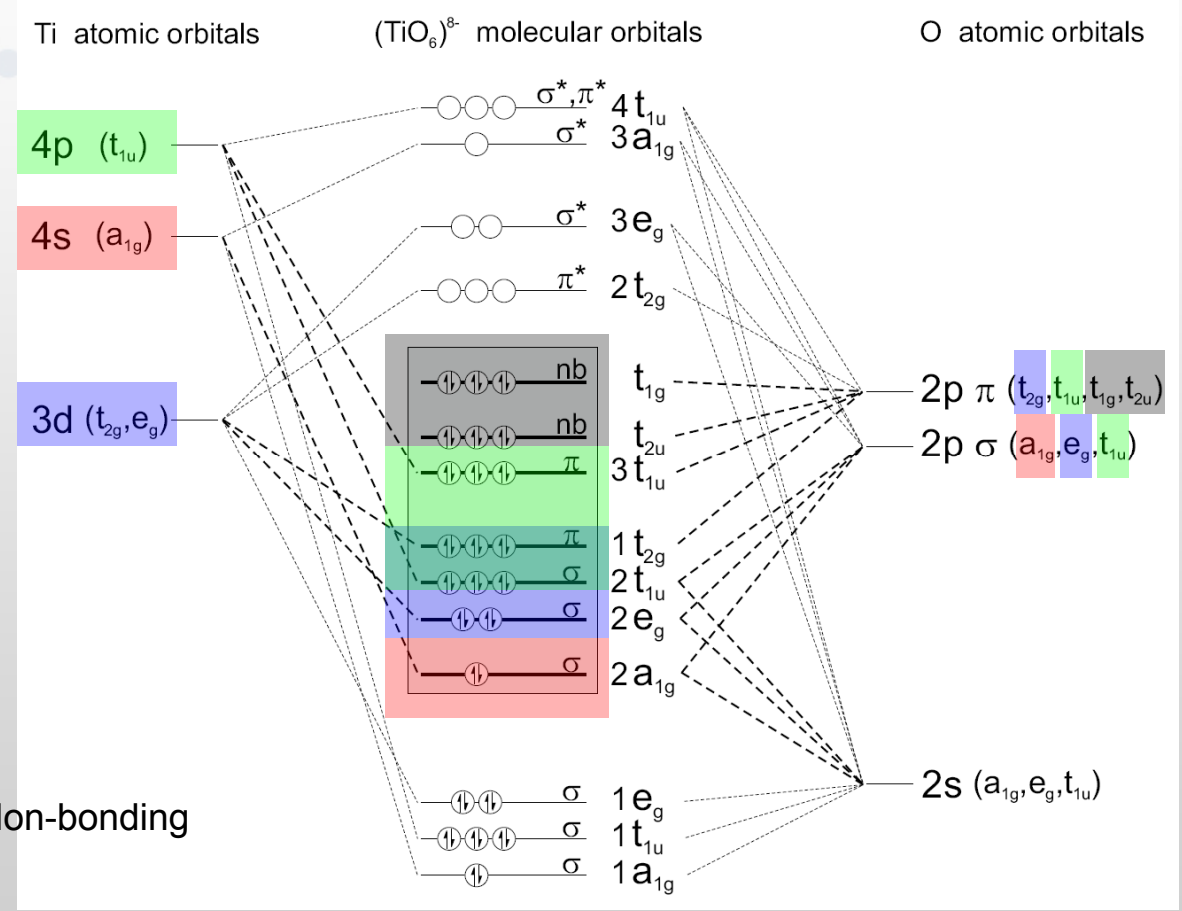

*Fischer, PRB **5**, 4219 (1972)*

Rutile TiO_2

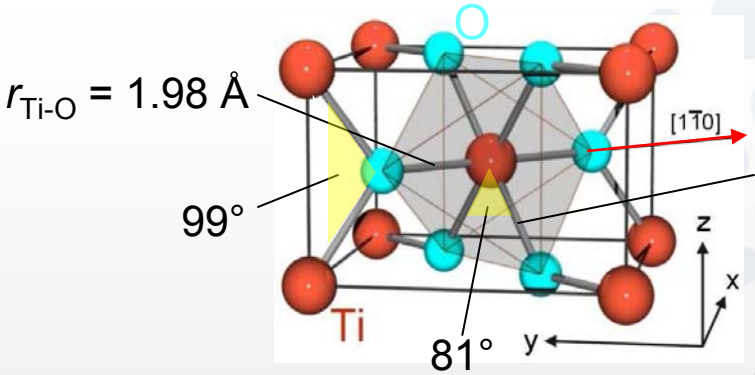

$SrTiO_3$

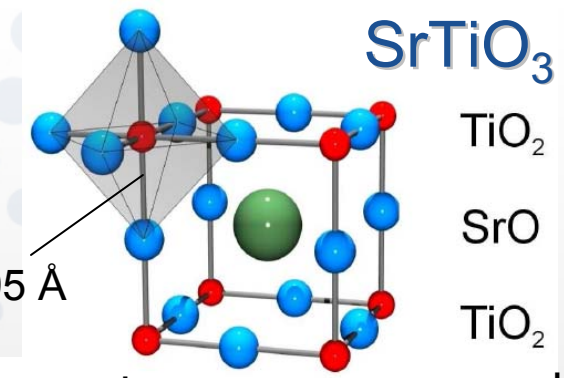

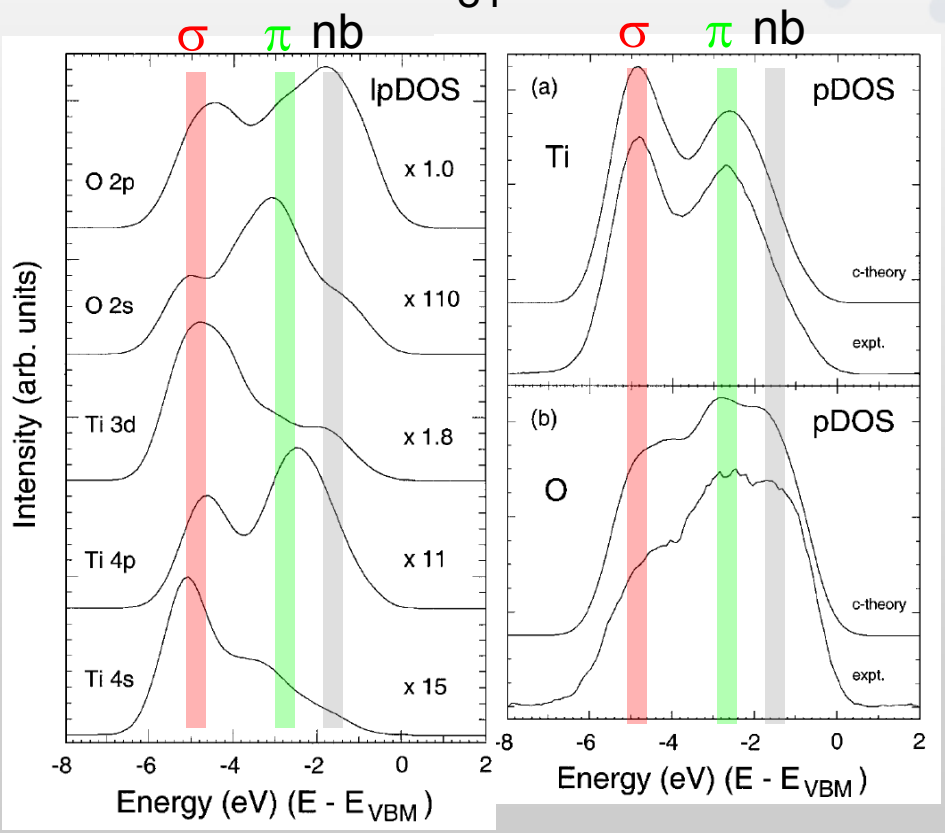

Woicik et al., PRL 89, 077401 (2002)

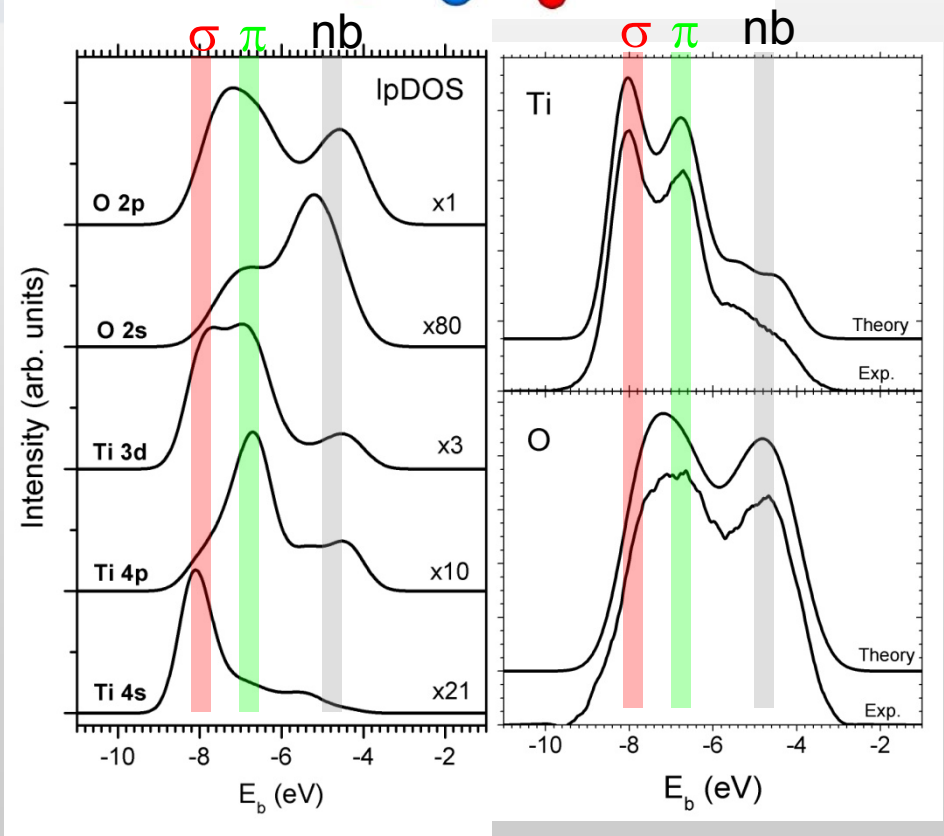

Present work

Broadening of $SrTiO_3$ valence band spectrum

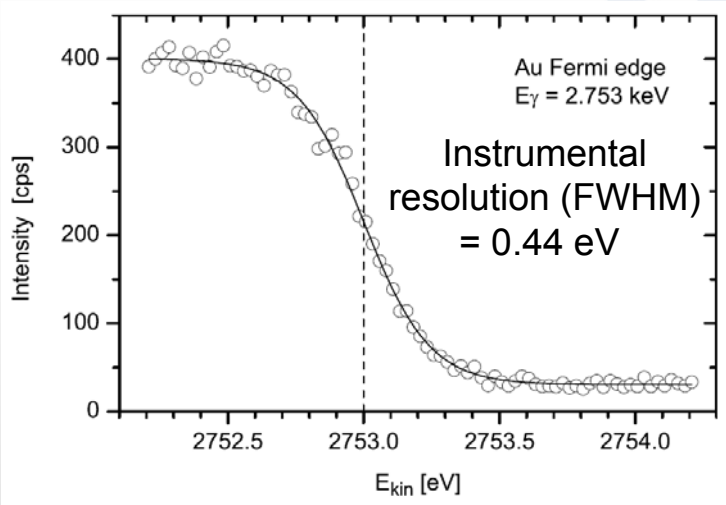

Chambers et al.

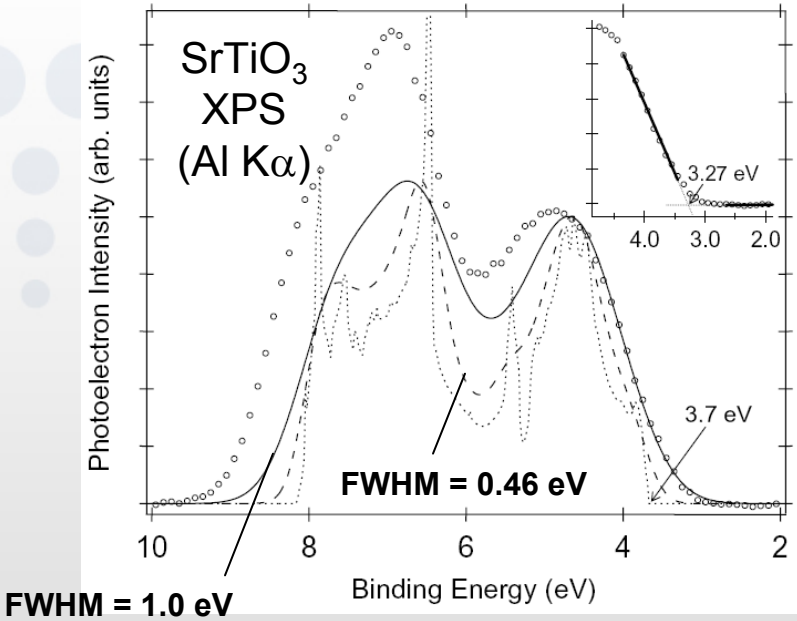

lpDOS convoluted with a Gaussian of FWHM = 0.44 eV

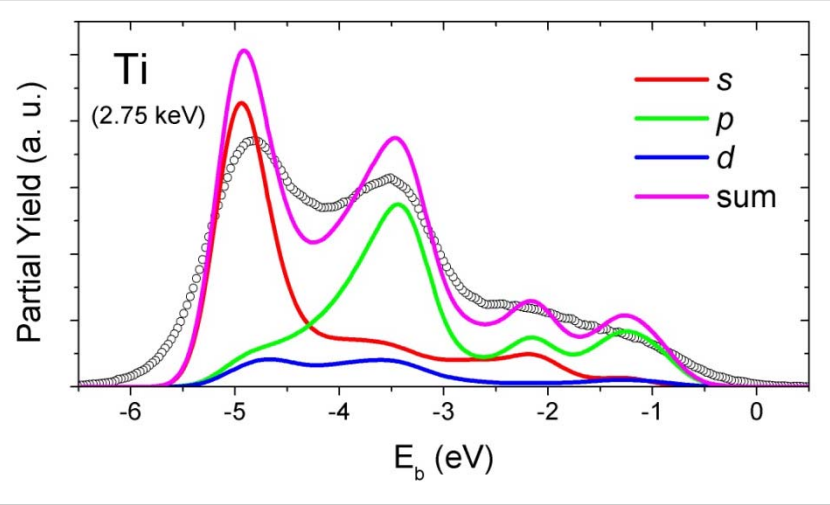

	Source	FWHM (eV) instrument	FWHM (eV) Gaussian
$BaTiO_3$	Al Kα	**0.6**	**1.2**
*Pertosa et al., PRB **18**, 5177 (1978)*			
$SrTiO_3$	Al Kα	**0.55**	**1.35**
*Wolfram & Ellialtioglu, PRB **19**, 43 (1979)*			
$SrTiO_3$	Al Kα	**0.46**	**1.0**
*Chambers et al., Surf. Sci. **554**, 81 (2004)*			
$SrTiO_3$	2.75 & 3.89 keV	**0.44**	**0.8**
Present work			